Position Control of a Cable-driven Dexterous Robotic Arm

Submitted by

Tran Le Dung

School of Mechanical and Aerospace Engineering

Nanyang Technological University

Undergraduate Research Opportunity Program (UROP)
project report

2009/2010

ABSTRACT

Dexterous robotic arms have gained increasing attention in the robotics community in recent years. The robotic arm with cable-driven parallel mechanism has many advantages instead of linkage such as: light-weight structure, low energy consumption, high speed motion due to low moment inertia and it is suitable to work in constrained work-conditions. Therefore, a lot of researchers spend their time and efforts to design an optimal structure for snake-like robotic arm supported by cable-driven parallel mechanism. This project also does not lie outside that trace. The objective is to design and implement the motion control on a cable-driven robotic arm. The position control of 2-module robotic arm is the main focus of project.

Through the kinematic and inverse kinematic analysis, the Labview program was used to write the commands for robotic system. Control system included: PID controller card that PID values could be determined by digital, continuous approaches as well as practical approach, amplifier to control the motion of Maxon servo DC motor, encoder used as feedback device to controller card. With proper hardware setup, the experiment for position control was conducted. It is shown that the cable-driven dexterous robotic arm can be controlled in a coordinated manner and follow a trajectory smoothly under position control. Some issues could be concerned in the future is the geometry for backbone, the design for actuation unit should be modified for more accurate cable-length's adjustments. With all of its applications, the developing in dexterous robotic arm using CDPM is very significant and important nowadays.

Keywords – Dexterous robotic arms, Cable-driven mechanism, Position control

ACKNOWLEDGEMENTS

I would like to express my heartfelt gratitude and deepest appreciation to all the people who had guided and taught me throughout the course of this project.

- **Associate Professor Yeo Song Huat**, who served as my UROP supervisor, for his time, concern and invaluable advices to motivate me.

- Appreciation is also extended to **Mr. Lim Wen Bin** and **Ms. Zhang Zhao** for their kind guidance.

- Appreciation to the staffs in SIMTech and Robotics Research Center for their help during my research period.

TABLE OF CONTENTS

LIST OF APPENDICES

LIST OF FIGURES

LIST OF TABLES

LIST OF GRAPHS

CHAPTER 1: INTRODUCTION

1.1. Background:

For recent years, almost researchers focus on design and analysis parallel mechanism combining with serial mechanism. Based on the configurations, parallel mechanism has unique advantages beside serial mechanism. In serial configuration, the drivers are connected in serial manner, in contrast all drivers in parallel manner are attaching on the base, hence the workload is divided equally between drivers. The other advantage is the parallel mechanism can achieve high velocity as well as high acceleration, the one that in serial manner is impossible [1].

With cable driven parallel mechanism (CDPM), using the cable to drive the platform, the redundancy of mechanism's weight makes the mechanism become simple, helping to reduce the inertial moment and the energy consumption [2]. But, the kinematic analysis of cable length required more efforts and the cable has always to be in the tensile state to avoid the sagging.

One of the most signification applications of CDPM is dexterous robotic arm. The cable-driven dexterous robotic arm in the research is a serial mechanism formed by parallel mechanism modules as shown in the Figure 1-1.

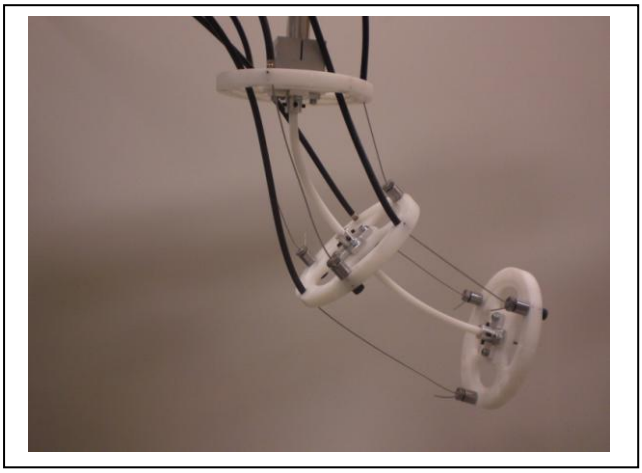

Figure 1-1: Cable-driven dexterous robotic arm

With advantages as mentioned previously, the snake-like robotic arm with the usage of CDPM becomes the key of our life. It can be developed and used in diverging fields such as:

- **Industry**
  - ❖ Nuclear: Decommissioning, Repair and maintenance [3][4]
  - ❖ Aerospace:
    - Manufacture and assembly: inside wing boxes, jet engines and ducts.
    - Surface Preparation: wielding pneumatic sanders for all stages of surface finishing prior to final paint application.
    - Maintenance, Repair and Overhaul
  - ❖ Automotive
    - Manufacture: Snake-arm robots allow structures to be assembled in a different way.
- **Security and defence**
  - Bomb disposal and counter terrorism [4]
  - Search and rescue [5]

Figure 1-2: snake-like robot in nuclear inspection [24]

Figure 1-3: snake-like robot in search and rescue [28]

All of above applications required high speed operation with high accuracy, deal in constrained workspace and replace the appearance of human. Therefore, the developing in dexterous robotic arm using CDPM is very significant and important nowadays. And the project is one part of this mission.

1.2. Objective and scope:

The objective of this project is to design and implement the motion control on a cable-driven robotic arm prototype using the software platform Labview.

The scope of this project will focus on the implementation of position control of 2-module cable-driven robotic arm. The kinematic and inverse kinematic of mechanism are evaluated using Euler's orientation representation. By kinematic analysis, the posture of robotic arm is determined based on the orientated angle inputted from labview. By inverse kinematic, the orientation angles can be determined to get the target posture for robotic arm. The pose (e.g. the step movement of modules) is driven by cable that control by servomotor. To obtain the fast and correct movement of motor, the PID controller is used with PID parameters determined from 2 approaches: practical approach (using Measurement & Automation Explorer (MAX)) and analytical method (with continuous and digital method). The algorithm for controlling motors simultaneously is based on the Labview software language. After the experiment conducted, the target position analysis and the speed of step movement are evaluated for the project's purposes.

1.2. Organization of the Report:

- Chapter 1 provides an introduction to CDPM and the motivation behind this project. The objectives and scope of the project are also defined in this chapter.
- Chapter 2 is the literature review. Including the research on different types of CDPM. Then, some brief introduction about the PID controller and step response, and end with discussion in various kinds of dexterous robotic arm.
- Chapter 3 describes the kinematic and inverse kinematic analysis for 2 as well as for n modules.
- Chapter 4 explains the design of position control systems. The chapter starts with a description of the hardware setup, follows by the software development that includes PID tuning and Labview program.
- Chapter 5 illustrates the experiment about movement of 1 module cable-driven dexterous robotic arm. With some discussion and evaluation about the movement accuracy of robotic arm.
- Chapter 6 concludes the project and provides suggestions for future work in this topic.

CHAPTER 2: LITERATURE REVIEW

This chapter will quickly give some information about the cable driven parallel mechanisms, motion control system, PID controller and design of dexterous robotic arms.

2.1. Cable Driven parallel mechanism:

Currently, most of robot manipulators' mechanisms are conventional mechanisms that consist of a number of rigid links and joints. Manipulator can be classified as 2 major types: serial and parallel according to kinematic analysis [6] [7]. Cable driven parallel mechanism is one of favorable form nowadays. CDPM is formed by replacing all the supporting legs of the parallel mechanism with cables. Many advantages in using cable instead of linkages are:

- Simple mechanical and light-weight structure, low energy consumption
- Large workspace, limited by cable lengths and cable tension constraints
- Low moment inertia and high speed motion (comparing with linkages and joints mechanism)
- Easy reconfigurability by relocating platform connecting points and base suspending points

So far, there are a lot of researches focusing on the CDPM such as workspace analysis and optimal design of cable-driven planar parallel manipulators [8], stiffness analysis [9], dynamic and control [10] [11], tension analysis in CDPM [12]. In general, CDPM is classified by 3 categories given by Ming and Higuchi [13] based on the number of cables (m) and number of DOF (n).

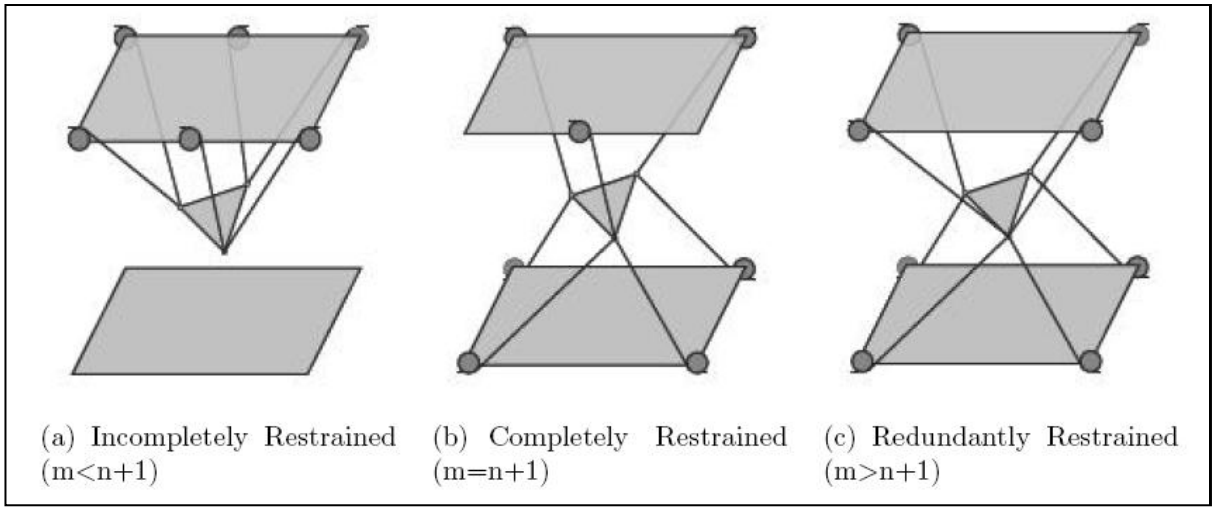

Figure 2-1: Classification of CDPM
based on the number of DOF (n) and number of cables (m) [13]

- When m < n+1, the system can be classified as incompletely restrained. The number of cables is not enough to conduct all the DOF required, so the external force such as gravity is required. Comparing to conventional parallel and serial mechanism, the robot can move easily with high energy efficiency. Skycam [11] is one of applications for this system, as shown in Figure 2-2.
- When m = n+1, the system is fully restrained
- When m > n+1, the system is redundantly restrained

In completely restrained and redundantly restrained systems, the pose can be completely determined by the function of cable lengths. The applications with high speed, high acceleration or high stiffness prefer using these configurations [14]. Increasing redundancy of CDPM will improve the stability of the system, however it requires more motors as well as lose DOF due to extra constrains [15].

Figure 2-2: Example of incompletely restrained CDPM-Skycam [16]

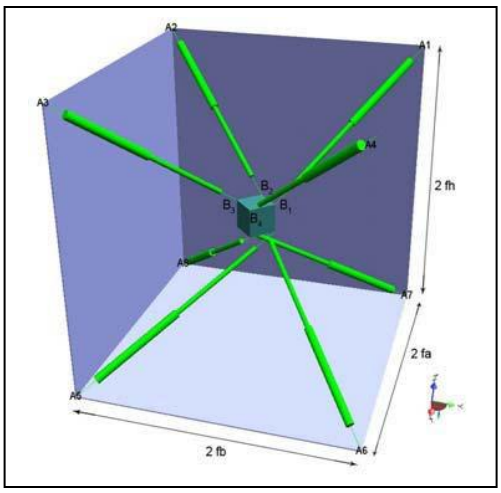

Figure 2-3: Example of redundantly constrained CDPM [17]

In this project, the CDPM with fully restrained configuration is used (with 3 cables control 1 module with 2 DOF).

2.2. PID controller:

PID controller (Proportional – integral – derivative controller) is a generic control loop feedback mechanism widely used in industrial control systems. A PID controller calculates an "error" value as the difference between a measured process variable and a desired setpoint. The controller attempts to minimize the error by adjusting the process control inputs. The PID controller calculation involves three separate parameters, and is accordingly sometimes called three-term control: the proportional, the integral and derivative values, denoted *P*, *I*, and *D*. It may also be necessary to alter the PID parameters depending on specific circumstances.[18]

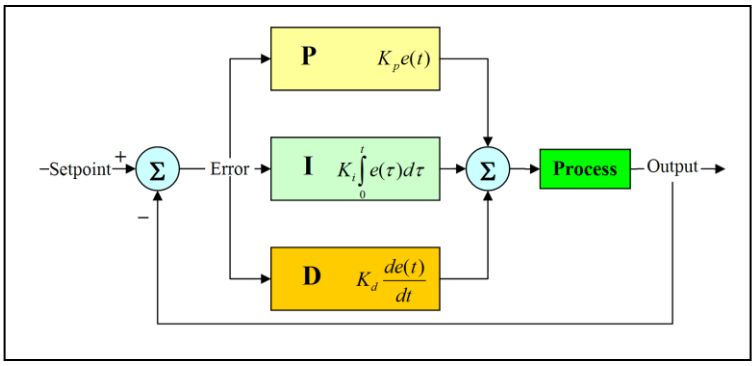

Figure 2-4: A block diagram of a PID controller [18]

PID CONTROL LOOP PARAMETERS:

Proportional Gain (Kp)—Proportional gain is the system **stiffness**. It determines the contribution of restoring force directly proportional to the position error. Restoring force is comparable to a spring in a mechanical system.

A high proportional gain gives a stiff responsive system but can cause instability from overshooting and oscillation.

Derivative Gain (Kd)—Derivative gain is the **damping** effects on the system. It determines the contribution of restoring force proportional to the rate of change (derivative) of position error. This force is much like viscous damping in a damped spring and mass mechanical system—a shock absorber, for example.

Increasing derivative gain reduces oscillation at the commanded position, or it rings because of high acceleration.

Integral Gain (Ki)—Integral gain is the **static torque** load on the system. It determines the contribution of restoring force that increases with time, ensuring that the

static position error in the servo loop is forced to 0. This restoring force works against constant torque loads to help achieve zero position error when an axis is stopped. Integral gain improves positional accuracy. High static torque loads need integral gains to minimize position error when stopped.

To determine the PID parameters, the step-response is used:

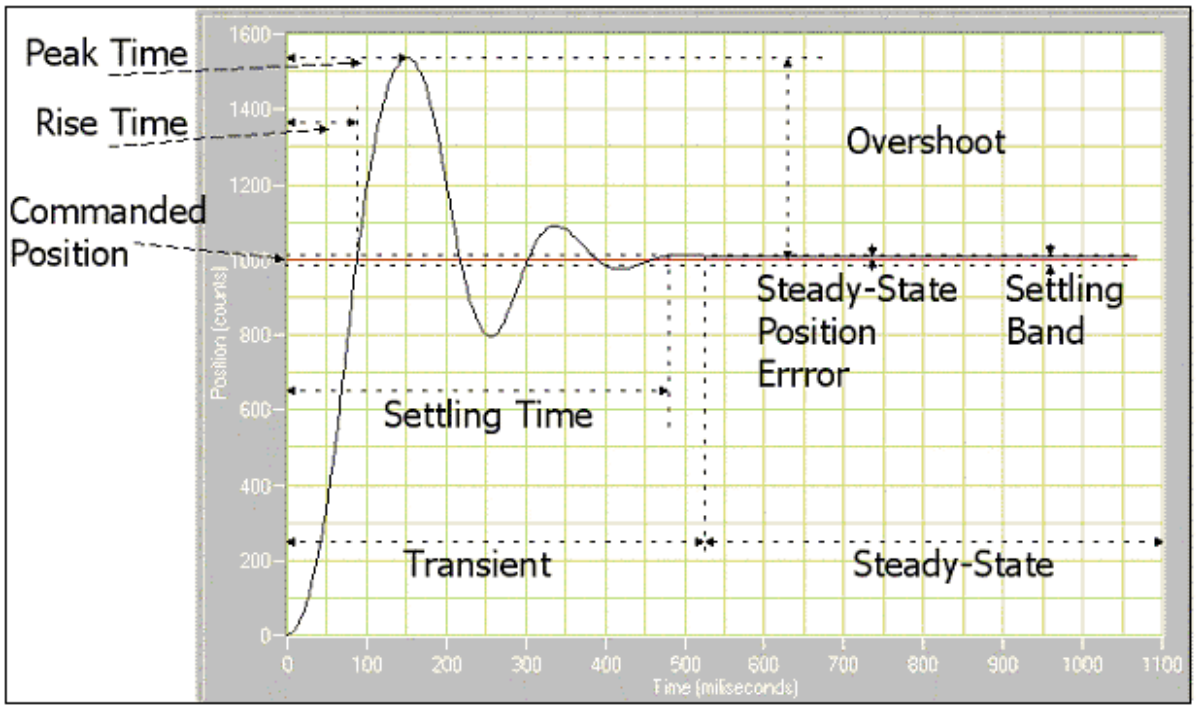

Figure 2-5: Step response [19]

Settling Time is the time required by the response curve to reach and stay within a range that is approximately the final value of size specified by the absolute percentage of the final value (2% to 5%).

Rise Time is the time required by the response to rise from 10% to 90% of its final value; the faster the response time of the system, the faster the rise time.

The optimal achieve when the overshoot, settling time and steady-state position error are small.

2.3. Dexterous robotic arm:

Dexterous robotic arms have gained increasing attention in the robotics community in recent years due to their high flexibility [20] [21] [22]. Over years, there are a lot of designs as well as researches focusing on the dexterous robotic arms.

The ESA Dextrous robot Arm (DexArm) [23] project is engaged in the design and development of a robot arm comparable in size, force capabilities and dexterity to a human arm, suitable for space applications. One set of design constraints for DexArm results from it having to withstand the harsh environment of space. Beyond these requirements however, the main challenges for the development team came with the minimization of resource usage. To achieve this goal, ESA has encouraged the use of innovative approaches and technologies to drastically reduce mass, volume and power consumption while providing adequate performance in terms of both torque/force capability and positioning accuracy and repeatability.

Figure 2.6: 3D rendering of DexArm design in action [23]

The other kind of dexterous robotic arm is snake-like robots. A snake like robot is typical example of a robot with redundant degree of freedom, and it can move also on narrow place and a place with a height difference. Many researchers discussed possibilities of the usage of such robots for disaster relief or dangerous zone work. There are a lot of designs have been conducted for snake robot. However the issue is in control this type of robot, the singular posture (the state when it is impossible for a robot to move further) should be avoided (control of locomotion and head configuration) (shown in Figures 2-7 and 2-8)

Figure 2-9: The snake-arm robots have more than 20 degrees of movement [24]

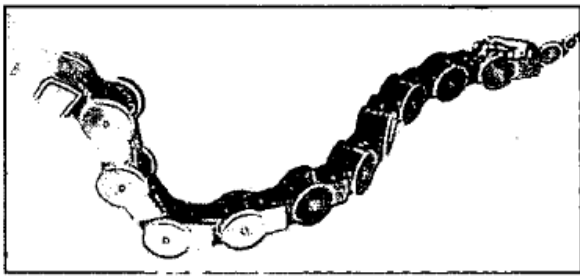

Figure 2-7: Super-Mechano Anaconda (SMA) robot [25]

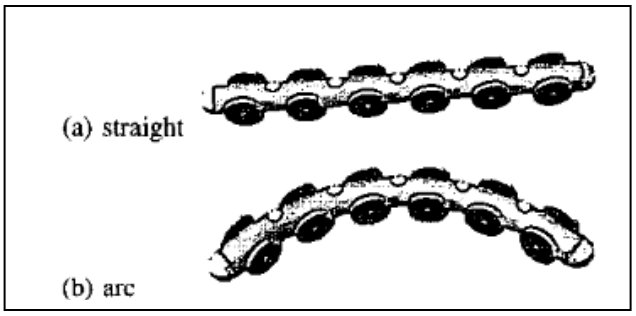

Figure 2.8: Singular posture of SMA robot [25]

Figure 2-7 and 2-9 show different designs of snake robot arm. There are two kinds of snake robots: discrete and continuous robot. The key advantage of using discrete robots is that the motion of the snake robot is predictable. However, its disadvantage is that they cannot provide high output speed. In contrast, due to their capability of bending continuously, continuum robots can achieve higher speeds relative to their discrete counterparts but the motion is unpredictable. Our target is design a robot that combines advantages of both: high output speed and predictable motion.

CHAPTER 3: KINEMATIC FORMULATION

3.1. Orientation representation

One of the basic problems in finding the 3-D orientation workspace is the choice of coordinates to describe the orientation of the mobile platform. Euler angle parameters (Yang and Haug, 1994) can be used to represent the mobile platform orientation. The main disadvantage is the existence of singularities at which the one-to-one correspondence between the actual orientation and the Euler angles does not hold.

The first requirements set for the Euler angles are met by the standard Euler angles that are defined by first rotating the mobile frame about the base z-axis by an angle ϕ, then about the mobile y'-axis by an angle θ, and finally about the mobile z'-axis by an angle ψ. For this choice of Euler angles, the singularity occurs at $\theta = 0^0$ and the rotation matrix is defined as:

$$R = R_z(\phi)R_{y'}(\theta)R_{z'}(\psi) = R_z(\phi)R_y(\theta)R_z(\psi)$$

The standard Euler angles give complicated plots of orientation workspace so a modified set of Euler angles were introduced. In new orientation representation, firstly, rotating the mobile platform about the base z-axis by an angle ϕ , then about the base y-axis by an angle θ , then about z-axis by an angle - ϕ ,and finally about the mobile z'-axis by an angle ψ. The singularity occurs at $\theta = 0^0$. Angle ψ is the "roll angle", angle θ is the "tilt angle", and angle ϕ is the angle between the base x-axis and the projection of the approach vector onto the base xy-plane

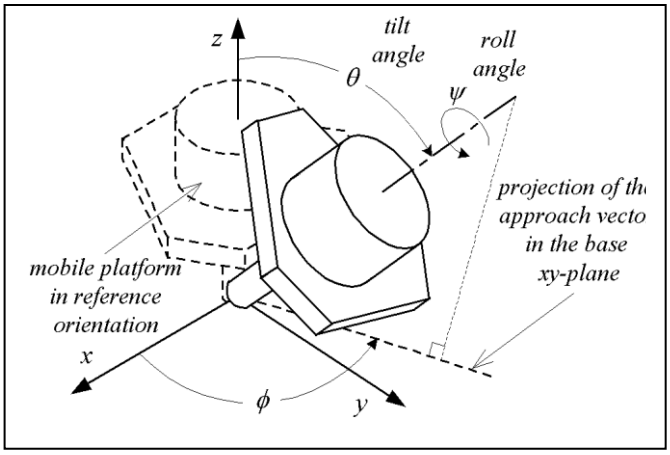

Figure 3-1: The modified Euler angles defining the platform orientation [26]

It should be noted that the roll angles ψ are equal to zero because assuming no torsional rotation. Therefore, the rotational matrix is defined as:

$$R = R_z(\phi)R_{y'}(\theta)R_z(-\phi)R_{z'}(\psi)$$

$$= R_z(\phi)R_y(\theta)R_z(\psi-\phi)$$

$$= R_z(\phi)R_y(\theta)R_z(-\phi)$$

The rotational transformation is defined as:

$$R_x(\alpha)=\begin{bmatrix}1 & 0 & 0\\ 0 & \cos\alpha & -\sin\alpha\\ 0 & \sin\alpha & \cos\alpha\end{bmatrix};\ R_y(\beta)=\begin{bmatrix}\cos\beta & 0 & \sin\beta\\ 0 & 1 & 0\\ -\sin\beta & 0 & \cos\beta\end{bmatrix};\ R_z(\gamma)=\begin{bmatrix}\cos\gamma & -\sin\gamma & 0\\ \sin\gamma & \cos\gamma & 0\\ 0 & 0 & 1\end{bmatrix}$$

Therefore:

$$R(\phi,\theta) = R_z(\phi)R_y(\theta)R_z(-\phi)$$

$$=\begin{bmatrix}\cos\phi & -\sin\phi & 0\\ \sin\phi & \cos\phi & 0\\ 0 & 0 & 1\end{bmatrix}\begin{bmatrix}\cos\theta & 0 & \sin\theta\\ 0 & 1 & 0\\ -\sin\theta & 0 & \cos\theta\end{bmatrix}\begin{bmatrix}\cos\phi & \sin\phi & 0\\ -\sin\phi & \cos\phi & 0\\ 0 & 0 & 1\end{bmatrix}$$

$$= \begin{bmatrix} (\cos^2\phi\cos\theta + \sin^2\phi) & (\cos\phi\cos\theta\sin\phi - \sin\phi\cos\phi) & (\cos\phi\sin\theta) \\ (\sin\phi\cos\theta\cos\phi - \cos\phi\sin\phi) & (\sin^2\phi\cos\theta + \cos^2\phi) & (\sin\phi\sin\theta) \\ (-\sin\theta\cos\phi) & (-\sin\theta\sin\phi) & \cos\theta \end{bmatrix}$$

3.2. Kinematic analyses:

The kinematic analysis of robotic arm is represented by following chart:

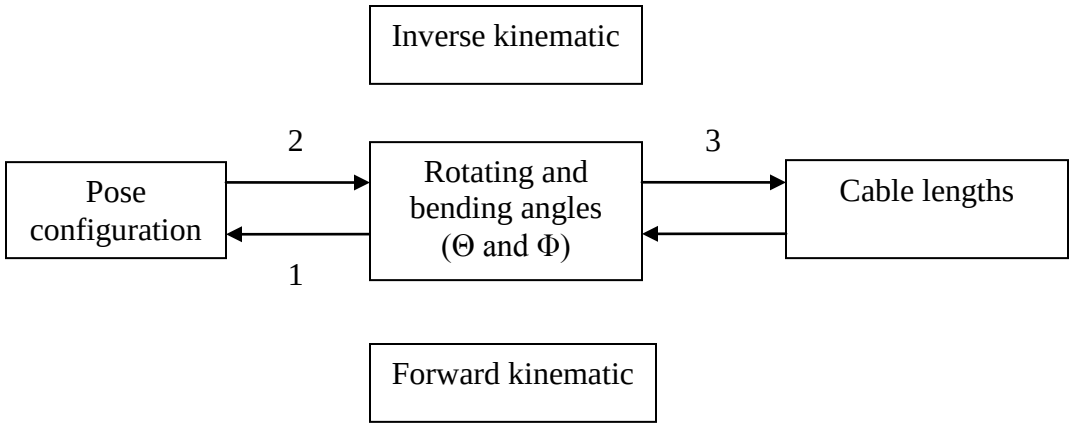

The report will represent inverse kinematic analysis (2 and 3) together with one part of forward kinematic analysis (1)

3.2.1. Forward kinematic:

Given the rotating and bending angles, the pose or the coordinates of endpoints will be determined.

Let the initial length of backbone be $2L_0$. Some assumptions should be made for state of module after movement with set of rotation and tilt angles (Φ,Θ):

- The length of backbone remains the same as $2L_0$ after movement of robotic arm
- The feature of module can be represented as the universal join with the length of each arm is L formulated based on the tilt angle and backbone length.(shown in the Figure 3-3)

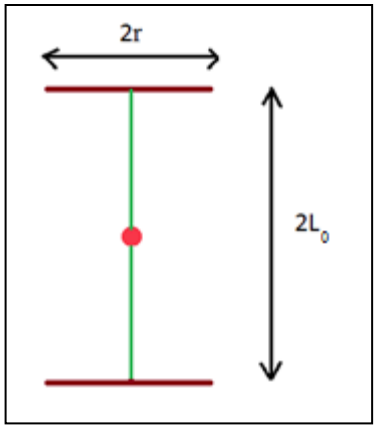

Figure 3-2: Module before movement

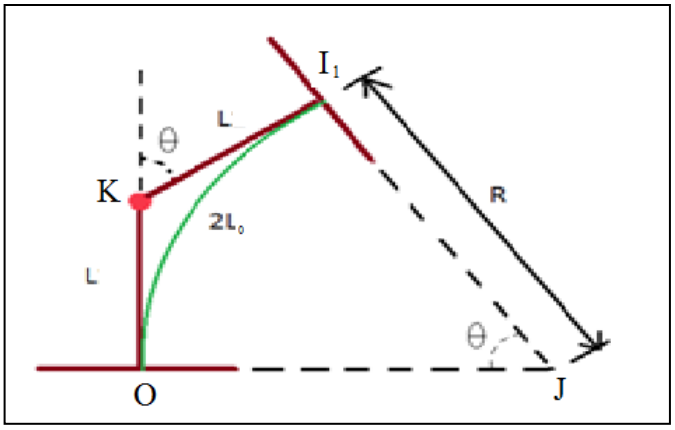

Figure 3-3: Module after movement

To formulate the equation for the length of universal joint, the bended backbone considered as arc of one circle with radius =R. So the length of arc is equal to

$$2L_0 = \frac{\theta}{2\pi} \times 2\pi R \qquad \rightarrow R = \frac{2L_0}{\theta}$$

Two sides of universal joint's module are always tangent to the bended backbone are, therefore angle $KI_1J = 90^0$

$$\tan\left(\frac{\theta}{2}\right) = \frac{L}{R}$$

The length of each arm in universal joint represented by

$$L = \frac{2L_0}{\theta}\tan\left(\frac{\theta}{2}\right)$$

1. For 2 modules:

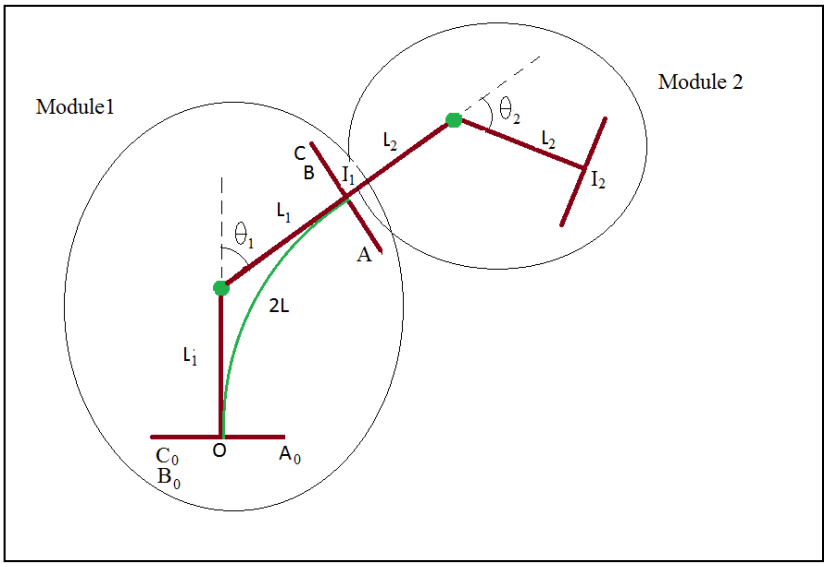

Figure 3-4: Modules 1 and 2 after movement

In which the rotating and bending angles of modules 1 and 2 respectively are (ϕ_1, θ_1) and (ϕ_2, θ_2)

Based on the previous analysis: $L_1 = \frac{2L_0}{\theta_1}\tan\left(\frac{\theta_1}{2}\right)$ and $L_2 = \frac{2L_0}{\theta_2}\tan\left(\frac{\theta_2}{2}\right)$

End-Point I_1 (Module1)

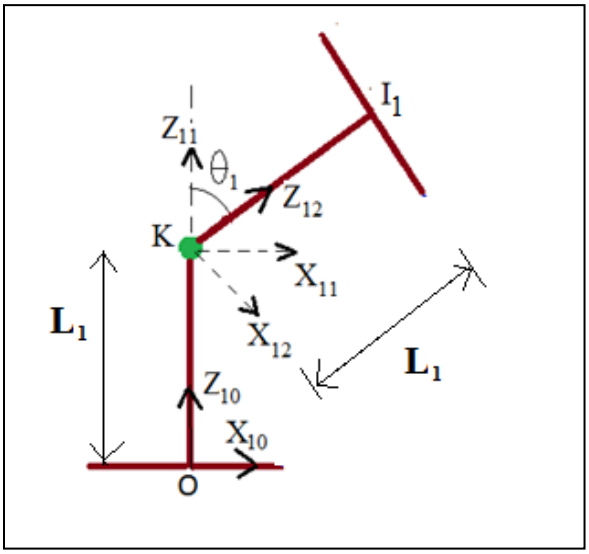

Figure 3-5: Coordinate systems of module 1

Frame 10 ($O_{10}X_{10}Y_{10}Z_{10}$) $\xrightarrow[(0\ \ 0\ \ L_1)]{translating}$ Frame 11($O_{11}X_{11}Y_{11}Z_{11}$) $\xrightarrow[(\phi_1,\theta_1)]{rotating}$ Frame 12($O_{12}X_{12}Y_{12}Z_{12}$)

Using transformation matrix from frame 12 to 10:

$$ {}^{10}_{12}T = {}^{10}_{11}Q\,{}^{11}_{12}R = \begin{bmatrix} I_{3x3} & \begin{pmatrix} 0 \\ 0 \\ L_1 \end{pmatrix} \\ 0 \quad 0 \quad 0 & 1 \end{bmatrix} \times \begin{bmatrix} R_{(\phi_1;\theta_1)} & 0 \\ 0 & 1 \end{bmatrix} = \begin{bmatrix} R_{(\phi_1;\theta_1)} & \begin{pmatrix} 0 \\ 0 \\ L_1 \end{pmatrix} \\ 0 \quad 0 \quad 0 & 1 \end{bmatrix} $$

Therefore, the coordinate of end-point I_1 in global coordinator corresponding to frame 10 is formulated as:

$$ {}^{10}\{I_1\} = {}^{10}_{12}T\,{}^{12}\{I_1\} $$

$$ = \begin{bmatrix} R_{(\phi_1;\theta_1)} & \begin{pmatrix} 0 \\ 0 \\ L_1 \end{pmatrix} \\ 0 \quad 0 \quad 0 & 1 \end{bmatrix} \times \begin{pmatrix} 0 \\ 0 \\ L_1 \\ 1 \end{pmatrix} = \begin{pmatrix} R_{(\phi_1;\theta_1)} \times \begin{pmatrix} 0 \\ 0 \\ L_1 \end{pmatrix} + \begin{pmatrix} 0 \\ 0 \\ L_1 \end{pmatrix} \\ 1 \end{pmatrix} $$

$$ \rightarrow {}^{10}\{I_1\} = R_{(\phi_1;\theta_1)} \times \begin{pmatrix} 0 \\ 0 \\ L_1 \end{pmatrix} + \begin{pmatrix} 0 \\ 0 \\ L_1 \end{pmatrix} = \begin{pmatrix} L_1 \cos\phi_1 \sin\theta_1 \\ L_1 \sin\phi_1 \sin\theta_1 \\ L_1 \cos\theta_1 + L_1 \end{pmatrix} $$

End-Point I_2 (Module2)

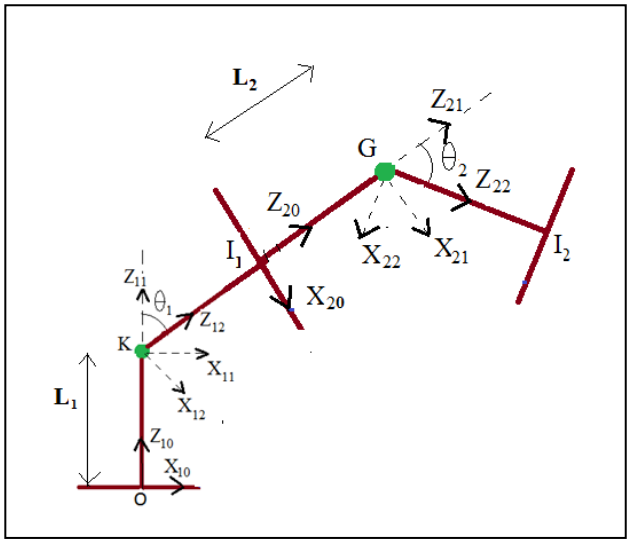

Figure 3-6: Coordinate systems of module 1 and 2

Frame 10 ($O_{10}X_{10}Y_{10}Z_{10}$) $\xrightarrow[(0\ \ 0\ \ L_1)]{translating}$ Frame 11 ($O_{11}X_{11}Y_{11}Z_{11}$) $\xrightarrow[(\phi_1,\theta_1)]{rotating}$

Frame 12($O_{12}X_{12}Y_{12}Z_{12}$) $\xrightarrow[(0\ \ 0\ \ L_1+L_2)]{translating}$ Frame 21($O_{21}X_{21}Y_{21}Z_{21}$) $\xrightarrow[(\phi_2,\theta_2)]{rotating}$

Frame 22($O_{22}X_{22}Y_{22}Z_{22}$)

Transformation matrix from frame 22 to 10:

$$
\begin{aligned}
{}^{10}_{22}T &= {}^{10}_{11}Q\,{}^{11}_{12}R\,{}^{12}_{21}Q\,{}^{21}_{12}R \\
&= \begin{bmatrix} I_{3x3} & \begin{pmatrix} 0 \\ 0 \\ L_1 \end{pmatrix} \\ 0 & 1 \end{bmatrix} \times \begin{bmatrix} R_{(\phi_1;\theta_1)} & 0 \\ 0 & 1 \end{bmatrix} \times \begin{bmatrix} I_{3x3} & \begin{pmatrix} 0 \\ 0 \\ L_1+L_2 \end{pmatrix} \\ 0 & 1 \end{bmatrix} \times \begin{bmatrix} R_{(\phi_2;\theta_2)} & 0 \\ 0 & 1 \end{bmatrix} \\
&= \begin{bmatrix} R_{(\phi_1;\theta_1)} & \begin{pmatrix} 0 \\ 0 \\ L_1 \end{pmatrix} \\ 0 & 1 \end{bmatrix} \times \begin{bmatrix} R_{(\phi_2;\theta_2)} & \begin{pmatrix} 0 \\ 0 \\ L_1+L_2 \end{pmatrix} \\ 0 & 1 \end{bmatrix} \\
&= \begin{pmatrix} R_{(\phi_1;\theta_1)} \times R_{(\phi_2;\theta_2)} & R_{(\phi_1;\theta_1)} \times \begin{pmatrix} 0 \\ 0 \\ L_1+L_2 \end{pmatrix} + \begin{pmatrix} 0 \\ 0 \\ L_1 \end{pmatrix} \\ 0 & 1 \end{pmatrix}
\end{aligned}
$$

Therefore, the coordinate of end-point I_2 in global coordinator corresponding to frame 10 is formulated as:

$$
\begin{aligned}
{}^{10}\{I_2\} &= {}^{10}_{22}T\,{}^{22}\{I_2\} \\
&= \begin{pmatrix} R_{(\phi_1;\theta_1)} \times R_{(\phi_2;\theta_2)} & R_{(\phi_1;\theta_1)} \times \begin{pmatrix} 0 \\ 0 \\ L_1+L_2 \end{pmatrix} + \begin{pmatrix} 0 \\ 0 \\ L_1 \end{pmatrix} \\ 0 & 1 \end{pmatrix} \times \begin{pmatrix} 0 \\ 0 \\ L_2 \\ 1 \end{pmatrix}
\end{aligned}
$$

$$= \begin{pmatrix} R_{(\phi_1:\theta_1)} \times R_{(\phi_2:\theta_2)} \times \begin{pmatrix} 0 \\ 0 \\ L_2 \end{pmatrix} + R_{(\phi_1:\theta_1)} \times \begin{pmatrix} 0 \\ 0 \\ L_1 + L_2 \end{pmatrix} + \begin{pmatrix} 0 \\ 0 \\ L_1 \end{pmatrix} \\ 1 \end{pmatrix}$$

Or:

$${}^{10}\{I_2\} = R_{(\phi_1:\theta_1)} \times R_{(\phi_2:\theta_2)} \times \begin{pmatrix} 0 \\ 0 \\ L_2 \end{pmatrix} + R_{(\phi_1:\theta_1)} \times \begin{pmatrix} 0 \\ 0 \\ L_1 + L_2 \end{pmatrix} + \begin{pmatrix} 0 \\ 0 \\ L_1 \end{pmatrix}$$

2. For n modules:

Assuming that there are n modules in configuration and the end-point in module n^{th} is I_n.

The formulating for coordinator of I_n is required.

There are 3 frames in one module n0, n1 and n2 based on the translation:

Frame n0 ($O_{n0}X_{n0}Y_{n0}Z_{n0}$) $\xrightarrow[(0 \quad 0 \quad L_n)]{translating}$ Frame n1 ($O_{n1}X_{n1}Y_{n1}Z_{n1}$)

$\xrightarrow[(\phi_n, \theta_n)]{rotating}$ Frame n2 ($O_{n2}X_{n2}Y_{n2}Z_{n2}$)

The length of universal joint's arm for each module presented by

$$L_n = \frac{2l}{\theta_n} \tan\left(\frac{\theta_n}{2}\right)$$

To determine the coordinator of end-point I_n in frame 10(the base-coordinator), the diagram used for convenience:

$$\{I_n\}_{10} \longleftrightarrow \{I_n\}_{11} \longleftrightarrow \{I_n\}_{12} \longleftrightarrow \{I_n\}_{22} \longleftrightarrow \{I_n\}_{32} \longleftrightarrow .... \{I_n\}_{(n-1)2} \longleftrightarrow \{I_n\}_{n2}$$

$$
\begin{aligned}
{}^{10}_{n2}T &= {}^{10}_{11}Q\,{}^{11}_{12}R\,{}^{12}_{21}Q\,{}^{21}_{12}R \ldots {}^{(n-1)2}_{n1}Q\,{}^{n1}_{n2}R \\
&= \begin{bmatrix} I_{3x3} & \begin{pmatrix} 0 \\ 0 \\ L_1 \end{pmatrix} \\ 0 \quad 0 & 1 \end{bmatrix} \times \begin{bmatrix} R_{(\phi_1;\theta_1)} & 0 \\ 0 & 1 \end{bmatrix} \times \begin{bmatrix} I_{3x3} & \begin{pmatrix} 0 \\ 0 \\ L_1 + L_2 \end{pmatrix} \\ 0 \quad 0 & 1 \end{bmatrix} \times \begin{bmatrix} R_{(\phi_2;\theta_2)} & 0 \\ 0 & 1 \end{bmatrix} \times \ldots \times \begin{bmatrix} I_{3x3} & \begin{pmatrix} 0 \\ 0 \\ L_{n-1} + L_n \end{pmatrix} \\ 0 \quad 0 & 1 \end{bmatrix} \times \begin{bmatrix} R_{(\phi_n;\theta_n)} & 0 \\ 0 & 1 \end{bmatrix} \\
&= \begin{bmatrix} R_{(\phi_1;\theta_1)} & \begin{pmatrix} 0 \\ 0 \\ L_1 \end{pmatrix} \\ 0 \quad 0 & 1 \end{bmatrix} \times \begin{bmatrix} R_{(\phi_2;\theta_2)} & \begin{pmatrix} 0 \\ 0 \\ L_1 + L_2 \end{pmatrix} \\ 0 \quad 0 & 1 \end{bmatrix} \times \ldots \times \begin{bmatrix} R_{(\phi_n;\theta_n)} & \begin{pmatrix} 0 \\ 0 \\ L_{n-1} + L_n \end{pmatrix} \\ 0 \quad 0 & 1 \end{bmatrix}
\end{aligned}
$$

The coordinate of end-point I_n in global coordinator corresponding to frame 10 is formulated as:

$$
\begin{aligned}
{}^{10}\{I_n\} &= {}^{10}_{n2}T\,{}^{n2}\{I_n\} \\
&= \begin{bmatrix} R_{(\phi_1;\theta_1)} & \begin{pmatrix} 0 \\ 0 \\ L_1 \end{pmatrix} \\ 0 \quad 0 & 1 \end{bmatrix} \times \begin{bmatrix} R_{(\phi_2;\theta_2)} & \begin{pmatrix} 0 \\ 0 \\ L_1 + L_2 \end{pmatrix} \\ 0 \quad 0 & 1 \end{bmatrix} \times \ldots \times \begin{bmatrix} R_{(\phi_n;\theta_n)} & \begin{pmatrix} 0 \\ 0 \\ L_{n-1} + L_n \end{pmatrix} \\ 0 \quad 0 & 1 \end{bmatrix} \times \begin{pmatrix} 0 \\ 0 \\ L_n \\ 1 \end{pmatrix}
\end{aligned}
$$

3.2.2. Inverse kinematics:

A/ Changing of cable lengths:

Given the rotating and bending angles, the purpose is to find the cable lengths.

A.1/ For 2 modules:

For this part, the 2-module robotic arm is considered

Analyzing the changes in cable length for:

- Module 1: Cables 1, 2, 3 corresponding to vectors $\overrightarrow{A_oA}, \overrightarrow{B_oB}$ and $\overrightarrow{C_oC}$
- Module 2: Cables 4, 5, 6 corresponding to vectors $\overrightarrow{D_oD}, \overrightarrow{E_oE}$ and $\overrightarrow{F_oF}$

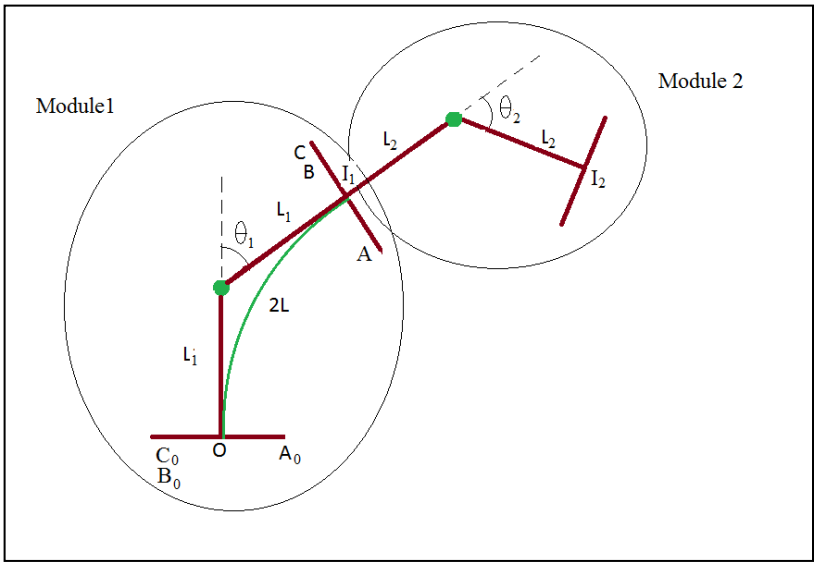

Figure 3-4: Modules 1 and 2 after movement

Module1: Assume that there are 3 frames in module 1 (shown as below figure) related by relationship:

Frame 10 $(O_{10}X_{10}Y_{10}Z_{10})$ $\xrightarrow[(0 \quad 0 \quad L1)]{translating}$ Frame 11$(O_{11}X_{11}Y_{11}Z_{11})$

$\xrightarrow[(\phi 1, \theta 1)]{rotating}$ Frame 12$(O_{12}X_{12}Y_{12}Z_{12})$

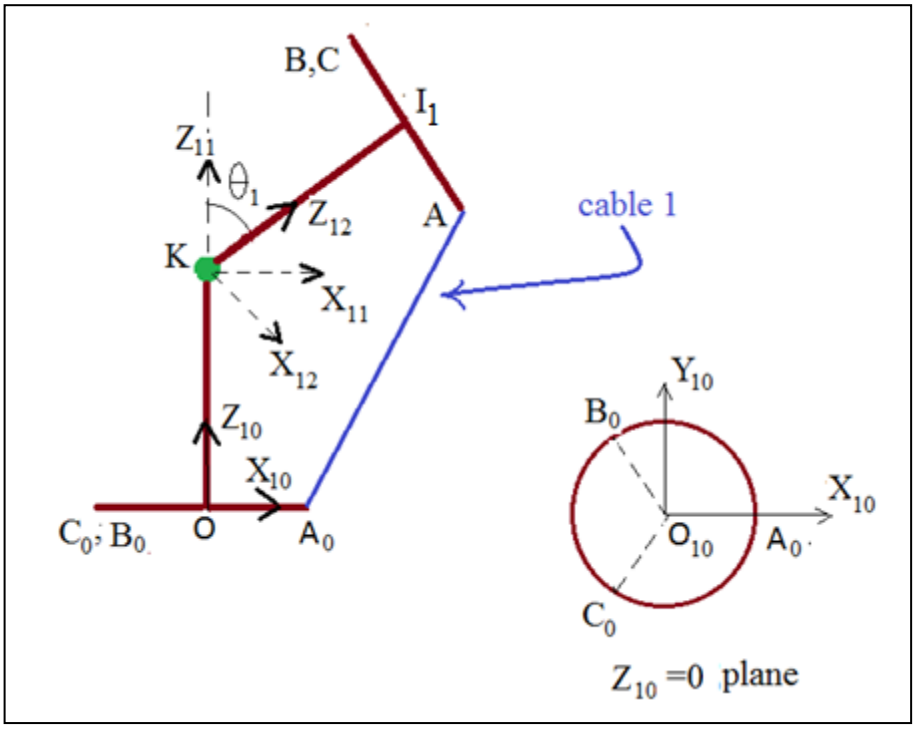

Figure 3-7: Module 1 after movement

$$\text{KO=KI}_1 = L_1 = \frac{2L_0}{\theta_1}\tan\left(\frac{\theta_1}{2}\right); \qquad \angle A_0O_{10}B_0 = \angle B_0O_{10}C_0 = \angle C_0O_{10}A_0 = 120^0$$

Transformation matrix from frame 12 to frame 10:

$${}^{10}_{12}T = {}^{10}_{11}Q\,{}^{11}_{12}R = \begin{bmatrix} I_{3x3} & \begin{pmatrix}0\\0\\L_1\end{pmatrix} \\ 0 \quad 1 \end{bmatrix} \times \begin{bmatrix} R_{(\phi_1;\theta_1)} & 0 \\ 0 & 1 \end{bmatrix} = \begin{bmatrix} R_{(\phi_1;\theta_1)} & \begin{pmatrix}0\\0\\L_1\end{pmatrix} \\ 0 \quad 1 \end{bmatrix}$$

Using the closed loop method to find the length of each cable after each movement.

- Cable1: Attach between 2 point A_0 and A. To find the length of cable 1, just take the magnitude of vector $\overrightarrow{A_oA}$

$$
\begin{aligned}
{}^{10}\{\overrightarrow{A_oA}\} &= {}^{10}\{\overrightarrow{A_oO}\} + {}^{10}\{\overrightarrow{OK}\} + {}^{10}\{\overrightarrow{KI_1}\} + {}^{10}\{\overrightarrow{I_1A}\} \\
{}^{10}\{\overrightarrow{A_oA}\} &= {}^{10}\{\overrightarrow{A_oO}\} + {}^{10}\{\overrightarrow{OK}\} + {}^{10}_{12}T \times {}^{12}\{\overrightarrow{KI_1}\} + {}^{10}_{12}T \times {}^{10}\{\overrightarrow{I_1A}\} \\
&= \begin{pmatrix} -r \\ 0 \\ 0 \\ 0 \end{pmatrix} + \begin{pmatrix} 0 \\ 0 \\ L_1 \\ 0 \end{pmatrix} + \begin{bmatrix} R_{(\phi_1;\theta_1)} & \begin{pmatrix} 0 \\ 0 \\ L_1 \end{pmatrix} \\ 0 \quad 0 \quad 0 & 1 \end{bmatrix} \times \begin{pmatrix} 0 \\ 0 \\ L_1 \\ 0 \end{pmatrix} + \begin{bmatrix} R_{(\phi_1;\theta_1)} & \begin{pmatrix} 0 \\ 0 \\ L_1 \end{pmatrix} \\ 0 \quad 0 \quad 0 & 1 \end{bmatrix} \times \begin{pmatrix} r \\ 0 \\ 0 \\ 0 \end{pmatrix} \\
&= \begin{pmatrix} -r \\ 0 \\ 0 \\ 0 \end{pmatrix} + \begin{pmatrix} 0 \\ 0 \\ L_1 \\ 0 \end{pmatrix} + \begin{pmatrix} R_{(\phi_1;\theta_1)} \times \begin{pmatrix} 0 \\ 0 \\ L_1 \end{pmatrix} \\ 0 \end{pmatrix} + \begin{pmatrix} R_{(\phi_1;\theta_1)} \times \begin{pmatrix} r \\ 0 \\ 0 \end{pmatrix} \\ 0 \end{pmatrix}
\end{aligned}
$$

The length of cable 1 after movement with set of rotation and tilt angles:

$$
\begin{aligned}
Cable1 = [&(-r + L_1\cos\phi\sin\theta + r\cos^2\phi\cos\theta + r\sin^2\phi)^2 + \\
&(L_1\sin\phi\sin\theta + r\sin\phi\cos\theta\cos\phi - r\cos\phi\sin\phi)^2 + (L_1 + L_1\cos\theta - r\sin\theta\cos\phi)^2]^{1/2}
\end{aligned}
$$

- Cable 2: Attach between 2 point B_0 and B. To find the length of cable 1, just take the magnitude of vector $\overrightarrow{B_0B}$

$$
\begin{aligned}
{}^{10}\{\overrightarrow{B_oB}\} &= {}^{10}\{\overrightarrow{B_oO}\} + {}^{10}\{\overrightarrow{OK}\} + {}^{10}\{\overrightarrow{KI_1}\} + {}^{10}\{\overrightarrow{I_1B}\} \\
{}^{10}\{\overrightarrow{B_oB}\} &= {}^{10}\{\overrightarrow{B_oO}\} + {}^{10}\{\overrightarrow{OK}\} + {}^{10}_{12}T \times {}^{12}\{\overrightarrow{KI_1}\} + {}^{10}_{12}T \times {}^{10}\{\overrightarrow{I_1B}\} \\
&= \begin{pmatrix} r\sin 30^0 \\ -r\cos 30^0 \\ 0 \\ 0 \end{pmatrix} + \begin{pmatrix} 0 \\ 0 \\ L_1 \\ 0 \end{pmatrix} + \begin{bmatrix} R_{(\phi_1;\theta_1)} & \begin{pmatrix} 0 \\ 0 \\ L_1 \end{pmatrix} \\ 0 \quad 0 \quad 0 & 1 \end{bmatrix} \times \begin{pmatrix} 0 \\ 0 \\ L_1 \\ 0 \end{pmatrix} + \begin{bmatrix} R_{(\phi_1;\theta_1)} & \begin{pmatrix} 0 \\ 0 \\ L_1 \end{pmatrix} \\ 0 \quad 0 \quad 0 & 1 \end{bmatrix} \times \begin{pmatrix} -r\sin 30^0 \\ r\cos 30^0 \\ 0 \\ 0 \end{pmatrix} \\
&= \begin{pmatrix} r\sin 30^0 \\ -r\cos 30^0 \\ 0 \\ 0 \end{pmatrix} + \begin{pmatrix} 0 \\ 0 \\ L_1 \\ 0 \end{pmatrix} + \begin{pmatrix} R_{(\phi_1;\theta_1)} \times \begin{pmatrix} 0 \\ 0 \\ L_1 \end{pmatrix} \\ 0 \end{pmatrix} + \begin{pmatrix} R_{(\phi_1;\theta_1)} \times \begin{pmatrix} -r\sin 30^0 \\ r\cos 30^0 \\ 0 \end{pmatrix} \\ 0 \end{pmatrix}
\end{aligned}
$$

$$Cable2 = \{[r\sin 30^0 + L_1\cos\phi\sin\theta - r\sin 30^0(\cos^2\phi\cos\theta + \sin^2\phi) + r\cos 30^0\sin\phi\cos\phi(\cos\theta - 1)]^2 +$$
$$[-r\cos 30^0 + L_1\sin\phi\sin\theta - r\sin 30^0\sin\phi\cos\phi(\cos\theta - 1) + r\cos 30^0(\sin^2\phi\cos\theta + \cos^2\phi)]^2 +$$
$$[L_1 + L_1\cos\theta + r\sin 30^0\sin\theta\cos\phi - r\cos 30^0\sin\theta\sin\phi]^2\}^{1/2}$$

- Cable 3: Attach between 2 point C_0 and C. To find the length of cable 1, just take the magnitude of vector $\overrightarrow{C_0C}$

$$^{10}\{\overrightarrow{C_oC}\} = {}^{10}\{\overrightarrow{C_oO}\} + {}^{10}\{\overrightarrow{OK}\} + {}^{10}\{\overrightarrow{KI_1}\} + {}^{10}\{\overrightarrow{I_1C}\}$$
$$^{10}\{\overrightarrow{C_oC}\} = {}^{10}\{\overrightarrow{C_oO}\} + {}^{10}\{\overrightarrow{OK}\} + {}^{10}_{12}T \times {}^{12}\{\overrightarrow{KI_1}\} + {}^{10}_{12}T \times {}^{10}\{\overrightarrow{I_1C}\}$$
$$= \begin{pmatrix} r\sin 30^0 \\ r\cos 30^0 \\ 0 \\ 0 \end{pmatrix} + \begin{pmatrix} 0 \\ 0 \\ L_1 \\ 0 \end{pmatrix} + \begin{bmatrix} R_{(\phi_1;\theta_1)} & \begin{pmatrix} 0 \\ 0 \\ L_1 \end{pmatrix} \\ 0 \quad 0 \quad 0 & 1 \end{bmatrix} \times \begin{pmatrix} 0 \\ 0 \\ L_1 \\ 0 \end{pmatrix} + \begin{bmatrix} R_{(\phi_1;\theta_1)} & \begin{pmatrix} 0 \\ 0 \\ L_1 \end{pmatrix} \\ 0 \quad 0 \quad 0 & 1 \end{bmatrix} \times \begin{pmatrix} -r\sin 30^0 \\ -r\cos 30^0 \\ 0 \\ 0 \end{pmatrix}$$
$$= \begin{pmatrix} r\sin 30^0 \\ r\cos 30^0 \\ 0 \\ 0 \end{pmatrix} + \begin{pmatrix} 0 \\ 0 \\ L_1 \\ 0 \end{pmatrix} + \begin{pmatrix} R_{(\phi_1;\theta_1)\times} \begin{pmatrix} 0 \\ 0 \\ L_1 \end{pmatrix} \\ 0 \end{pmatrix} + \begin{pmatrix} R_{(\phi_1;\theta_1)\times} \begin{pmatrix} -r\sin 30^0 \\ r\cos 30^0 \\ 0 \end{pmatrix} \\ 0 \end{pmatrix}$$

$$Cable3 = \{[r\sin 30^0 + L_1\cos\phi\sin\theta - r\sin 30^0(\cos^2\phi\cos\theta + \sin^2\phi) + r\cos 30^0\sin\phi\cos\phi(\cos\theta - 1)]^2 +$$
$$[r\cos 30^0 + L_1\sin\phi\sin\theta - r\sin 30^0\sin\phi\cos\phi(\cos\theta - 1) + r\cos 30^0(\sin^2\phi\cos\theta + \cos^2\phi)]^2 +$$
$$[L_1 + L_1\cos\theta + r\sin 30^0\sin\theta\cos\phi - r\cos 30^0\sin\theta\sin\phi]^2\}^{1/2}$$

Module2: Assume that there are 3 frames in module 2 (shown as below figure) related by relationship:

Frame 12 ($O_{12}X_{12}Y_{12}Z_{12}$) $\xrightarrow[(0 \quad 0 \quad L1)]{translating}$ Frame 20 ($O_{20}X_{20}Y_{20}Z_{20}$) $\xrightarrow[(0 \quad 0 \quad L_2)]{translating}$

Frame 21 ($O_{21}X_{21}Y_{21}Z_{21}$) $\xrightarrow[(\phi_2,\theta_2)]{rotating}$ Frame 22 ($O_{22}X_{22}Y_{22}Z_{22}$)

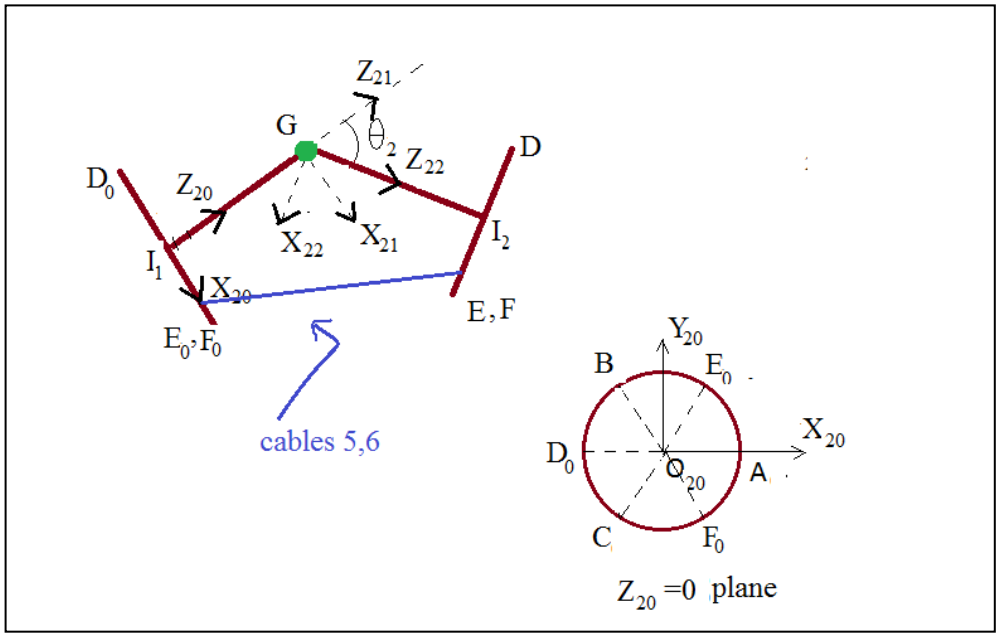

Figure 3-8: Module 2 after movement

$$I_1G=GI_2=L_2=\frac{2L_0}{\theta_2}\tan\left(\frac{\theta_2}{2}\right); \qquad \angle D_0O_{20}E_0=\angle E_0O_{20}F_0=\angle F_0O_{20}D_0=120^0$$

Transformation matrix from frame 22 to 20

$$^{20}_{22}T={}^{20}_{21}Q\,{}^{21}_{22}R=\begin{bmatrix} I_{3x3} & \begin{pmatrix}0\\0\\L_2\end{pmatrix} \\ 0 \quad 0 \quad 1 & \end{bmatrix}\times\begin{bmatrix} R_{(\phi_2;\theta_2)} & 0 \\ 0 & 1\end{bmatrix}=\begin{bmatrix} R_{(\phi_2;\theta_2)} & \begin{pmatrix}0\\0\\L_2\end{pmatrix} \\ 0 \quad 0 \quad 1 & \end{bmatrix}$$

- Cable 4: Attach between 2 point D_0 and D. To find the length of cable 1, just take the magnitude of vector $\overrightarrow{D_0D}$

$$^{20}\{\overrightarrow{D_oD}\}={}^{20}\{\overrightarrow{D_oI_1}\}+{}^{20}\{\overrightarrow{I_1G}\}+{}^{20}\{\overrightarrow{GI_2}\}+{}^{20}\{\overrightarrow{I_2D}\}$$
$$^{20}\{\overrightarrow{D_oD}\}={}^{20}\{\overrightarrow{D_oI_1}\}+{}^{20}\{\overrightarrow{I_1G}\}+{}^{20}_{22}T\times{}^{22}\{\overrightarrow{GI_2}\}+{}^{20}_{22}T\times{}^{20}\{\overrightarrow{I_2D}\}$$

$$= \begin{pmatrix} r \\ 0 \\ 0 \\ 0 \end{pmatrix} + \begin{pmatrix} 0 \\ 0 \\ L_2 \\ 0 \end{pmatrix} + \begin{bmatrix} R_{(\phi_2;\theta_2)} & \begin{pmatrix} 0 \\ 0 \\ L_2 \end{pmatrix} \\ 0 \quad 0 \quad 1 \end{bmatrix} \times \begin{pmatrix} 0 \\ 0 \\ L_2 \\ 0 \end{pmatrix} + \begin{bmatrix} R_{(\phi_2;\theta_2)} & \begin{pmatrix} 0 \\ 0 \\ L_2 \end{pmatrix} \\ 0 \quad 0 \quad 1 \end{bmatrix} \times \begin{pmatrix} -r \\ 0 \\ 0 \\ 0 \end{pmatrix}$$

$$= \begin{pmatrix} r \\ 0 \\ 0 \\ 0 \end{pmatrix} + \begin{pmatrix} 0 \\ 0 \\ L_2 \\ 0 \end{pmatrix} + \begin{pmatrix} R_{(\phi_2;\theta_2)\times} \begin{pmatrix} 0 \\ 0 \\ L_2 \end{pmatrix} \\ 0 \end{pmatrix} + \begin{pmatrix} R_{(\phi_2;\theta_2)\times} \begin{pmatrix} -r \\ 0 \\ 0 \end{pmatrix} \\ 0 \end{pmatrix}$$

- Cable 5: Attach between 2 point E_0 and E. To find the length of cable 1, just take the magnitude of vector $\overrightarrow{E_0E}$

$${}^{20}\{\overrightarrow{E_oE}\} = {}^{20}\{\overrightarrow{E_oI_1}\} + {}^{20}\{\overrightarrow{I_1G}\} + {}^{20}\{\overrightarrow{GI_2}\} + {}^{20}\{\overrightarrow{I_2E}\}$$

$${}^{20}\{\overrightarrow{E_oE}\} = {}^{20}\{\overrightarrow{E_oI_1}\} + {}^{20}\{\overrightarrow{I_1G}\} + {}^{20}_{22}T \times {}^{22}\{\overrightarrow{GI_2}\} + {}^{20}_{22}T \times {}^{20}\{\overrightarrow{I_2E}\}$$

$$= \begin{pmatrix} -r\sin 30^0 \\ -r\cos 30^0 \\ 0 \\ 0 \end{pmatrix} + \begin{pmatrix} 0 \\ 0 \\ L_2 \\ 0 \end{pmatrix} + \begin{bmatrix} R_{(\phi_2;\theta_2)} & \begin{pmatrix} 0 \\ 0 \\ L_2 \end{pmatrix} \\ 0 \quad 0 \quad 1 \end{bmatrix} \times \begin{pmatrix} 0 \\ 0 \\ L_2 \\ 0 \end{pmatrix} + \begin{bmatrix} R_{(\phi_2;\theta_2)} & \begin{pmatrix} 0 \\ 0 \\ L_2 \end{pmatrix} \\ 0 \quad 0 \quad 1 \end{bmatrix} \times \begin{pmatrix} r\sin 30^0 \\ r\cos 30^0 \\ 0 \\ 0 \end{pmatrix}$$

$$= \begin{pmatrix} -r\sin 30^0 \\ -r\cos 30^0 \\ 0 \\ 0 \end{pmatrix} + \begin{pmatrix} 0 \\ 0 \\ L_2 \\ 0 \end{pmatrix} + \begin{pmatrix} R_{(\phi_2;\theta_2)\times} \begin{pmatrix} 0 \\ 0 \\ L_2 \end{pmatrix} \\ 0 \end{pmatrix} + \begin{pmatrix} R_{(\phi_2;\theta_2)\times} \begin{pmatrix} r\sin 30^0 \\ r\cos 30^0 \\ 0 \end{pmatrix} \\ 0 \end{pmatrix}$$

- Cable 6: Attach between 2 point F_0 and F. To find the length of cable 1, just take the magnitude of vector $\overrightarrow{F_0F}$

$${}^{20}\{\overrightarrow{F_oF}\} = {}^{20}\{\overrightarrow{F_oI_1}\} + {}^{20}\{\overrightarrow{I_1G}\} + {}^{20}\{\overrightarrow{GI_2}\} + {}^{20}\{\overrightarrow{I_2F}\}$$

$${}^{20}\{\overrightarrow{F_oF}\} = {}^{20}\{\overrightarrow{F_oI_1}\} + {}^{20}\{\overrightarrow{I_1G}\} + {}^{20}_{22}T \times {}^{22}\{\overrightarrow{GI_2}\} + {}^{20}_{22}T \times {}^{20}\{\overrightarrow{I_2F}\}$$

$$= \begin{pmatrix} -r\sin 30^0 \\ r\cos 30^0 \\ 0 \\ 0 \end{pmatrix} + \begin{pmatrix} 0 \\ 0 \\ L_2 \\ 0 \end{pmatrix} + \begin{bmatrix} R_{(\phi_2;\theta_2)} & \begin{pmatrix} 0 \\ 0 \\ L_2 \end{pmatrix} \\ 0 \quad 0 \quad 1 \end{bmatrix} \times \begin{pmatrix} 0 \\ 0 \\ L_2 \\ 0 \end{pmatrix} + \begin{bmatrix} R_{(\phi_2;\theta_2)} & \begin{pmatrix} 0 \\ 0 \\ L_2 \end{pmatrix} \\ 0 \quad 0 \quad 1 \end{bmatrix} \times \begin{pmatrix} r\sin 30^0 \\ -r\cos 30^0 \\ 0 \\ 0 \end{pmatrix}$$

$$= \begin{pmatrix} -r\sin 30^0 \\ -r\cos 30^0 \\ 0 \\ 0 \end{pmatrix} + \begin{pmatrix} 0 \\ 0 \\ L_2 \\ 0 \end{pmatrix} + \begin{pmatrix} R_{(\phi_2;\theta_2)\times} \begin{pmatrix} 0 \\ 0 \\ L_2 \end{pmatrix} \\ 0 \end{pmatrix} + \begin{pmatrix} R_{(\phi_2;\theta_2)\times} \begin{pmatrix} r\sin 30^0 \\ r\cos 30^0 \\ 0 \end{pmatrix} \\ 0 \end{pmatrix}$$

A.2/ For n modules:

- With n is odd the change in length of 3 cables can be formulated similarly as module 1, so the length of each cable is the modulus of each vectors:

$$Vector1 = \begin{pmatrix} -r \\ 0 \\ 0 \end{pmatrix} + \begin{pmatrix} 0 \\ 0 \\ L_n \end{pmatrix} + R_{(\phi_n;\theta_n)} \begin{pmatrix} 0 \\ 0 \\ L_n \end{pmatrix} + R_{(\phi_n;\theta_n)} \begin{pmatrix} r \\ 0 \\ 0 \end{pmatrix}$$

$$Vector2 = \begin{pmatrix} r\sin 30^0 \\ -r\cos 30^0 \\ 0 \end{pmatrix} + \begin{pmatrix} 0 \\ 0 \\ L_n \end{pmatrix} + R_{(\phi_n;\theta_n)} \begin{pmatrix} 0 \\ 0 \\ L_n \end{pmatrix} + R_{(\phi_n;\theta_n)} \begin{pmatrix} -r\sin 30^0 \\ r\cos 30^0 \\ 0 \end{pmatrix}$$

$$Vector3 = \begin{pmatrix} r\sin 30^0 \\ r\cos 30^0 \\ 0 \end{pmatrix} + \begin{pmatrix} 0 \\ 0 \\ L_n \end{pmatrix} + R_{(\phi_n;\theta_n)} \begin{pmatrix} 0 \\ 0 \\ L_n \end{pmatrix} + R_{(\phi_n;\theta_n)} \begin{pmatrix} -r\sin 30^0 \\ -r\cos 30^0 \\ 0 \end{pmatrix}$$

- With n is even the change in length of 3 cables can be formulated similarly as module 2, so the length of each cable is the modulus of each vectors:

$$Vector4 = \begin{pmatrix} r \\ 0 \\ 0 \end{pmatrix} + \begin{pmatrix} 0 \\ 0 \\ L_n \end{pmatrix} + R_{(\phi_n;\theta_n)} \begin{pmatrix} 0 \\ 0 \\ L_n \end{pmatrix} + R_{(\phi_n;\theta_n)} \begin{pmatrix} -r \\ 0 \\ 0 \end{pmatrix}$$

$$Vector5 = \begin{pmatrix} -r\sin 30^0 \\ -r\cos 30^0 \\ 0 \end{pmatrix} + \begin{pmatrix} 0 \\ 0 \\ L_n \end{pmatrix} + R_{(\phi_n;\theta_n)} \begin{pmatrix} 0 \\ 0 \\ L_n \end{pmatrix} + R_{(\phi_n;\theta_n)} \begin{pmatrix} r\sin 30^0 \\ r\cos 30^0 \\ 0 \end{pmatrix}$$

$$Vector6 = \begin{pmatrix} -r\sin 30^0 \\ r\cos 30^0 \\ 0 \end{pmatrix} + \begin{pmatrix} 0 \\ 0 \\ L_n \end{pmatrix} + R_{(\phi_n;\theta_n)} \begin{pmatrix} 0 \\ 0 \\ L_n \end{pmatrix} + R_{(\phi_n;\theta_n)} \begin{pmatrix} r\sin 30^0 \\ -r\cos 30^0 \\ 0 \end{pmatrix}$$

B/ Rotating and bending angles:

Given the pose configuration, the purpose is to find the rotating and bending angles of all modules.

B.1. For 2 modules: Given the coordinates of end-points I_1(module 1) $\left(x_{I_1}, y_{I_1}, z_{I_1}\right)$, and I_2(module 2) $\left(x_{I_2}, y_{I_2}, z_{I_2}\right)$ find the rotation and tilt angles of module 1 and 2.

End-Point I_1: $$^{10}\{I\} = R_{(\phi_1;\theta_1)} \begin{pmatrix} 0 \\ 0 \\ L_1 \end{pmatrix} + \begin{pmatrix} 0 \\ 0 \\ L_1 \end{pmatrix}$$

$$LHS = \begin{pmatrix} x_{I_1} \\ y_{I_1} \\ z_{I_1} \end{pmatrix} \qquad RHS = \begin{pmatrix} L_1\cos\phi_1\sin\theta_1 \\ L_1\sin\phi_1\sin\theta_1 \\ L_1\cos\theta_1 + L_1 \end{pmatrix} \qquad \rightarrow \begin{pmatrix} x_{I_1} \\ y_{I_1} \\ z_{I_1} \end{pmatrix} = \begin{pmatrix} L_1\cos\phi_1\sin\theta_1 \\ L_1\sin\phi_1\sin\theta_1 \\ L_1\cos\theta_1 + L_1 \end{pmatrix}$$

The values of Φ_1 and Θ_1 determined as:

$$\boxed{\phi_1 = \tan^{-1}\left(\frac{y_{I_1}}{x_{I_1}}\right)} \text{and } \frac{y_{I_1}}{z_{I_1}} = \frac{\sin\phi_1\sin\theta_1}{\cos\theta_1 + 1}$$

$$\rightarrow \frac{\sin^2\theta_1}{(\cos\theta_1+1)^2} = A \text{ with } A = (\frac{y_{I_{10}}}{z_{I_{10}}}\sin\phi_1)^2$$

$$\rightarrow (A+1)\cos^2\theta_1 + 2A\cos\theta_1 + A - 1 = 0$$

$$\rightarrow \cos\theta_1 = \frac{-A+1}{A+1} \text{ so } \boxed{\theta_1 = \cos^{-1}(\frac{-A+1}{A+1})}$$

End-Point I_2:

$$
\begin{aligned}
{}^{10}\{I_2\} &= {}^{10}_{22}T\,{}^{22}\{I_2\} \\
&= \begin{bmatrix} R_{(\phi_1;\theta_1)} & \begin{pmatrix} 0 \\ 0 \\ L_1 \end{pmatrix} \\ 0 \quad 0 \quad 0 & 1 \end{bmatrix} \times \begin{bmatrix} R_{(\phi_2;\theta_2)} & \begin{pmatrix} 0 \\ 0 \\ L_1+L_2 \end{pmatrix} \\ 0 \quad 0 \quad 0 & 1 \end{bmatrix} \begin{pmatrix} 0 \\ 0 \\ L_2 \\ 1 \end{pmatrix} = \begin{pmatrix} x_{I_2} \\ z_{I_2} \\ z_{I_2} \\ 1 \end{pmatrix}
\end{aligned}
$$

$$
\begin{bmatrix} R_{(\phi_1;\theta_1)} & \begin{pmatrix} 0 \\ 0 \\ L_1 \end{pmatrix} \\ 0 \quad 0 \quad 0 & 1 \end{bmatrix}^{-1} \begin{pmatrix} x_{I_2} \\ z_{I_2} \\ z_{I_2} \\ 1 \end{pmatrix} = \begin{bmatrix} R_{(\phi_2;\theta_2)} & \begin{pmatrix} 0 \\ 0 \\ L_1+L_2 \end{pmatrix} \\ 0 \quad 0 \quad 0 & 1 \end{bmatrix} \begin{pmatrix} 0 \\ 0 \\ L_2 \\ 1 \end{pmatrix} = \begin{pmatrix} R_{(\phi_2;\theta_2)} \times \begin{pmatrix} 0 \\ 0 \\ L_2 \end{pmatrix} + \begin{pmatrix} 0 \\ 0 \\ L_1+L_2 \end{pmatrix} \\ 1 \end{pmatrix}
$$

From inverse kinematic analysis of point I_1 the values of set (ϕ_1, θ_1, L_1) can be determined

$$
\text{Let} \begin{bmatrix} R_{(\phi_1;\theta_1)} & \begin{pmatrix} 0 \\ 0 \\ L_1 \end{pmatrix} \\ 0 \quad 0 \quad 0 & 1 \end{bmatrix}^{-1} \begin{pmatrix} x_{I_2} \\ z_{I_2} \\ z_{I_2} \\ 1 \end{pmatrix} - \begin{pmatrix} 0 \\ 0 \\ L_1 \\ 0 \end{pmatrix} = \begin{pmatrix} x_2 \\ y_2 \\ z_2 \\ 1 \end{pmatrix} \text{ so } \begin{pmatrix} x_2 \\ y_2 \\ z_2 \\ 1 \end{pmatrix} = \begin{pmatrix} L_2 \cos\phi_2 \sin\theta_2 \\ L_2 \sin\phi_2 \sin\theta_2 \\ L_2 \cos\theta_2 + L_2) \\ 1 \end{pmatrix}
$$

The values of Φ_2 and $\Theta 2$ determined as:

$$
\boxed{\rightarrow \phi_2 = \tan^{-1}\left(\frac{y_2}{x_2}\right)} \text{and } \frac{y_2}{z_2} = \frac{\sin\phi_2 \sin\theta_2}{\cos\theta_2 + 1}
$$

$$
\rightarrow \frac{\sin^2\theta_2}{(\cos\theta_2+1)^2} = B \text{ with } B = (\frac{y_2}{z_2}\sin\phi_2)^2
$$

$$
\rightarrow (B+1)\cos^2\theta_2 + 2B\cos\theta_2 + B - 1 = 0
$$

$$
\rightarrow \cos\theta_2 = \frac{-B+1}{B+1} \text{ so } \boxed{\theta_2 = \cos^{-1}(\frac{-B+1}{B+1})}
$$

B.2. For n modules: Given the coordinates of all end-points of all modules: $\mathrm{I_i}\left(x_{I_1}, y_{I_1}, z_{I_1}\right)$ with $(i=\overline{1,n})$ find the torsion and tilt angles of all modules

$$
\begin{aligned}
{}^{10}\{I_n\} &= {}^{10}_{n2}T\,{}^{n2}\{I_n\} \\
&= \begin{bmatrix} R_{(\phi_1;\theta_1)} & \begin{pmatrix} 0 \\ 0 \\ L_1 \end{pmatrix} \\ 0 & 1 \end{bmatrix} \times \begin{bmatrix} R_{(\phi_2;\theta_2)} & \begin{pmatrix} 0 \\ 0 \\ L_1+L_2 \end{pmatrix} \\ 0 & 1 \end{bmatrix} \times \ldots \times \begin{bmatrix} R_{(\phi_n;\theta_n)} & \begin{pmatrix} 0 \\ 0 \\ L_{n-1}+L_n \end{pmatrix} \\ 0 & 1 \end{bmatrix} \times \begin{pmatrix} 0 \\ 0 \\ L_n \\ 1 \end{pmatrix} = \begin{pmatrix} x_{I_n} \\ y_{I_n} \\ z_{I_n} \\ 1 \end{pmatrix}
\end{aligned}
$$

Assuming all the sets: (ϕ_i, θ_i, L_i) with $(i=\overline{1,n-1})$ are determined by considering inverse kinematic analysis with end-effectors I_i with $(i=\overline{1,n-1})$. To determine the set (ϕ_n, θ_n, L_n) the inverse kinematic analysis is used.

$$
\begin{bmatrix} R_{(\phi_{n-1};\theta_{n-1})} & \begin{pmatrix} 0 \\ 0 \\ L_{n-2}+L_{n-1} \end{pmatrix} \\ 0 & 1 \end{bmatrix}^{-1} \times \ldots \times \begin{bmatrix} R_{(\phi_2;\theta_2)} & \begin{pmatrix} 0 \\ 0 \\ L_1+L_2 \end{pmatrix} \\ 0 & 1 \end{bmatrix}^{-1} \times \begin{bmatrix} R_{(\phi_1;\theta_1)} & \begin{pmatrix} 0 \\ 0 \\ L_1 \end{pmatrix} \\ 0 & 1 \end{bmatrix}^{-1} \times \begin{pmatrix} x_{I_n} \\ y_{I_n} \\ z_{I_n} \\ 1 \end{pmatrix}
$$

$$
= \begin{bmatrix} R_{(\phi_n;\theta_n)} & \begin{pmatrix} 0 \\ 0 \\ L_{n-1}+L_n \end{pmatrix} \\ 0 & 1 \end{bmatrix} \times \begin{pmatrix} 0 \\ 0 \\ L_n \\ 1 \end{pmatrix} = \begin{pmatrix} R_{(\phi_n;\theta_n)} \times \begin{pmatrix} 0 \\ 0 \\ L_n \end{pmatrix} + \begin{pmatrix} 0 \\ 0 \\ L_{n-1}+L_n \end{pmatrix} \\ 1 \end{pmatrix} = \begin{pmatrix} L_n \cos\phi_n \sin\theta_n \\ L_n \sin\phi_n \sin\theta_n \\ L_n(\cos\theta_n + 1) \\ 1 \end{pmatrix} + \begin{pmatrix} 0 \\ 0 \\ L_{n-1} \\ 0 \end{pmatrix}
$$

$$
\rightarrow \begin{pmatrix} L_n \cos\phi_n \sin\theta_n \\ L_n \sin\phi_n \sin\theta_n \\ L_n(\cos\theta_n + 1) \\ 1 \end{pmatrix} = \begin{pmatrix} x_n \\ y_n \\ z_n \\ 1 \end{pmatrix} \quad \text{in which}
$$

$$
\begin{pmatrix} x_n \\ y_n \\ z_n \\ 1 \end{pmatrix} = \begin{bmatrix} R_{(\phi_{n-1};\theta_{n-1})} & \begin{pmatrix} 0 \\ 0 \\ L_{n-2}+L_{n-1} \end{pmatrix} \\ 0 & 1 \end{bmatrix}^{-1} \times \ldots \times \begin{bmatrix} R_{(\phi_2;\theta_2)} & \begin{pmatrix} 0 \\ 0 \\ L_1+L_2 \end{pmatrix} \\ 0 & 1 \end{bmatrix}^{-1} \times \begin{bmatrix} R_{(\phi_1;\theta_1)} & \begin{pmatrix} 0 \\ 0 \\ L_1 \end{pmatrix} \\ 0 & 1 \end{bmatrix}^{-1} \times \begin{pmatrix} x_{I_n} \\ y_{I_n} \\ z_{I_n} \\ 1 \end{pmatrix} - \begin{pmatrix} 0 \\ 0 \\ L_{n-1} \\ 0 \end{pmatrix}
$$

known

$$\boxed{\rightarrow \phi_n = \tan^{-1}\left(\frac{y_n}{x_n}\right)} \text{and } \frac{y_n}{z_n} = \frac{\sin\phi_n \sin\theta_n}{\cos\theta_n + 1}$$

$$\rightarrow \frac{\sin^2\theta_n}{(\cos\theta_n + 1)^2} = C \text{ with } C = (\frac{y_n}{z_n}\sin\phi_n)^2$$

$$\rightarrow (C+1)\cos^2\theta_n + 2C\cos\theta_n + C - 1 = 0$$

$$\rightarrow \cos\theta_n = \frac{-C+1}{C+1} \quad \boxed{\rightarrow \theta_n = \cos^{-1}(\frac{-C+1}{C+1})}$$

The purpose of this inverse kinematic is: in application, once the target position of end-effector is determined, all the parameters such as tilt and rotation angles of each module should be clarified to conduct the motion of robotic arm.

CHAPTER 4: POSITION CONTROL SYSTEM

4.1. Overview:

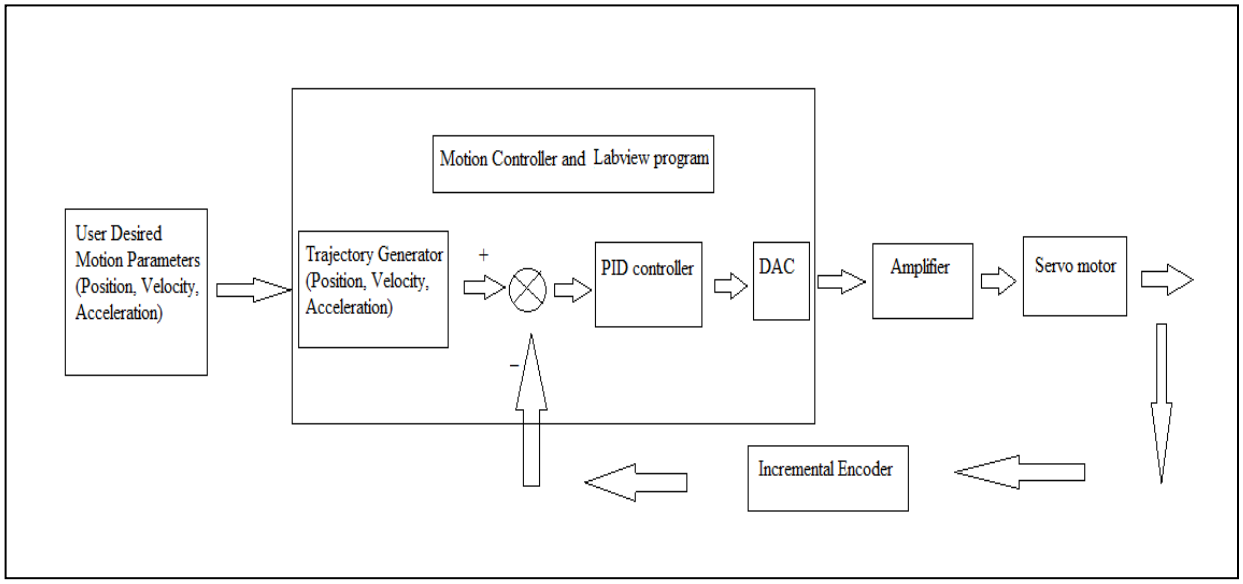

Figure 4-1: Position Control Loop

The position controlled motion system operates based on the incremental encoder feedback. This kind of feedback returns the current position. In this project, the controller is assigned with PID gains by the author will drive the motion of servo motor. Initially, author will set trajectory constraints in MAX and they become the maximum values of motion parameter including: position, velocity, acceleration and jerk. The NI motion controller is used to control the motion of servo motor. Once, all the constraints parameters were commanded, NI controller will create "Trajectory Generation" to make sure that the motion will be operated properly to get the target position. With PID assigned by author, the controller will manipulate the position error that is the difference between the desired position and actual position to maintain the required motion. The amplifier receives signal from PID controller in Voltage (Controller using DAC to convert digital signal to analo-

gue signal before sending to amplifier) and provides corresponding current to run the motor. The incremental encoder is attached in shaft of motor to record the current position of motor and to send the feedback into controller for adjustment the commanded signal that will provide desired position.

4.2. Position control setup:

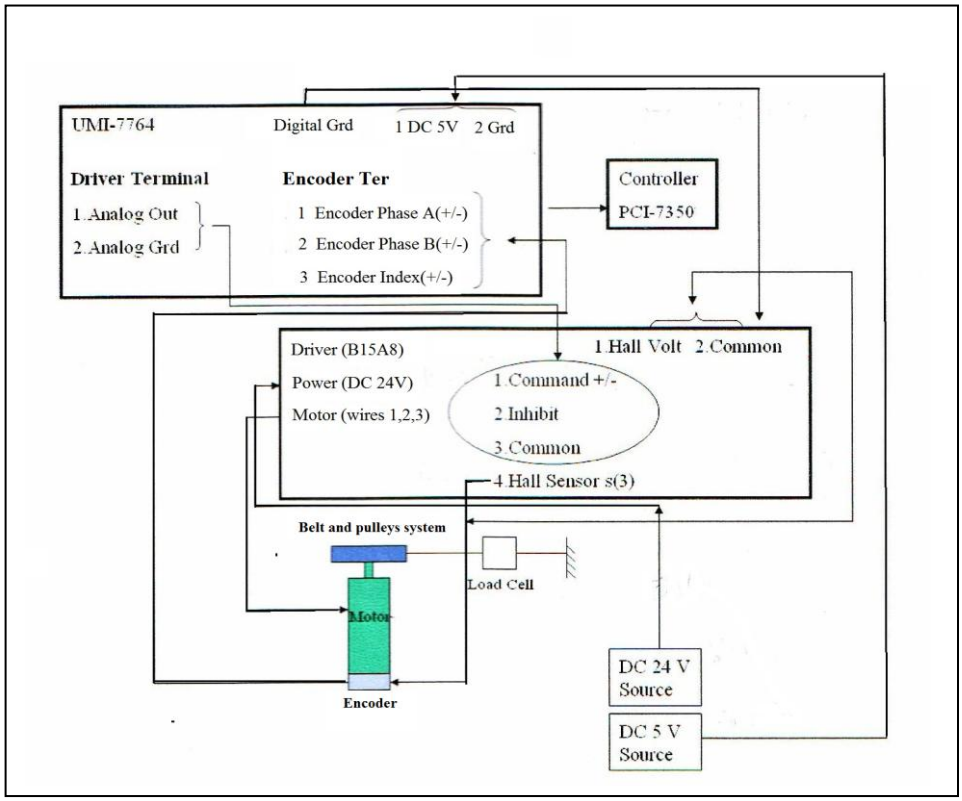

Figure 4-2: Position control setup wiring diagram

4.2.1. Hardware:

The prototype of dexterous robotic arm with one module is shown in the figure. Two ends of backbone is attached with holder part along with platform (radius = 50mm). To control the movement of one module with 2 DOF, there are necessarily 3 cables attached between 2 platforms. For 2 modules robotic arm, 6 cables are required to control the

movement. Each cable will connect with one actuation unit that including: motor, belt reduction (ratio=4), gearbox, and encoder that will send position feedback to controller. Along the chain way, gather with actuation are amplifier, controller card, connection box and computer with NI User Interface. The computer acts as the input source and relays the signal from the controller card inside computer to the controller board. The controller board as being an address receives the signal from encoder and then sends back to controller card, as well as being middle-terminal to transfer signal from controller card to amplifier to run the motor.

1. **Actuation unit**: comprises motor, drum, gearbox

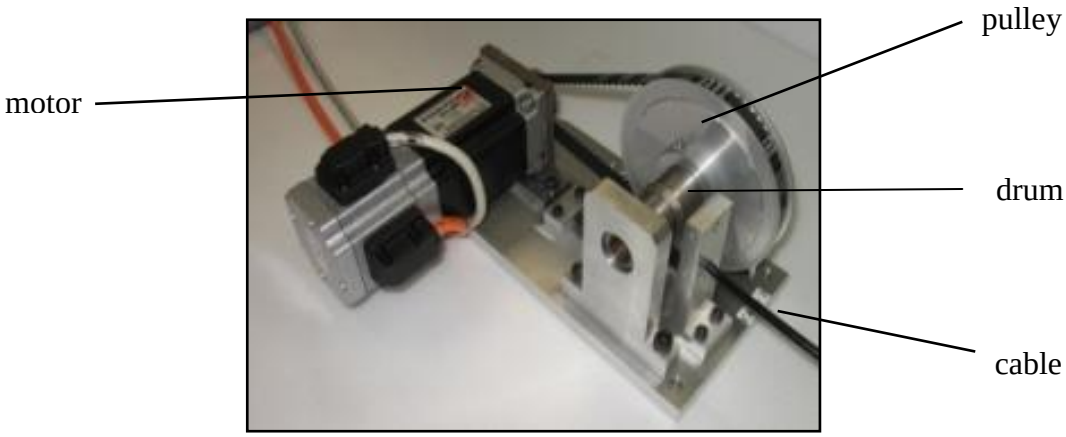

Figure 4-3: Actuation unit for one cable

The advantages of using brushless servomotor over stepper motors and brushed servo motor include maintenance-free, high torque, high speed and better controllability. The following table shows these differences between them.

	Pros	Cons	Applications
Stepper Motors	Inexpensive, can be run open loop, good low-end torque, clean rooms	Noisy and resonant, poor high-speed torque, not for hot environments, not for variable loads	Positioning, micromovement
Brushed DC Servo Motors	Inexpensive, moderate speed, good high-end torque, simple drives	Maintenance required, no clean rooms, brush sparking causes EMI and danger in explosive environments	Velocity control, high-speed position control
Brushless Servo Motors	Maintenance-free, long lifetime, no sparking, high speeds, clean rooms, quiet, run cool	Expensive and complicated drives	Robotics, pick-and-place, high-torque applications

Table 4-1: Comparisons between three kinds of motors

So the brushless DC servomotor is best choice for controlling the cable in CDPM. Brushless DC servomotors (EC 45-136198) from Maxon are selected as the actuator for this project. As the motor rotates, the driven sheave in the belt-drive will cause the respective cable to wrap up on the shaft. Some specifications of the motor are:

			136198
Motor Data			
	Values at nominal voltage		
1	Nominal voltage	V	24.0
2	No load speed	rpm	6070
3	No load current	mA	409
4	Nominal speed	rpm	4860
5	Nominal torque (max. continuous torque)	mNm	179
6	Nominal current (max. continuous current)	A	5.10
7	Stall torque	mNm	965
8	Starting current	A	26.0
9	Max. efficiency	%	77
	Characteristics		
10	Terminal resistance phase to phase	Ω	0.923
11	Terminal inductance phase to phase	mH	0.275
12	Torque constant	mNm / A	37.1
13	Speed constant	rpm / V	257
14	Speed / torque gradient	rpm / mNm	6.39
15	Mechanical time constant	ms	7.97
16	Rotor inertia	gcm²	119

Table 4-2: Specifications of motor

They are 150W/24V DC servomotors with no load speed of 6070 rpm. Each motor are attached to a planetary gear head with 2 stages reduction ratio of 26 and 81% efficiency. With this stages reduction, the configuration will increase the amount of torque supplied to the driven shaft by 26 times. Due to the increase in torque, the cables will be able to exert a larger pulling force on the cable-driven dexterous robotic arm.

2. Encoder:

An electrical mechanical device that converts linear or rotary displacement into digital pulse signals. An optical encoder consists of a rotating disk, a light source, and a photodetector (light sensor). The disk, which is mounted on the rotating shaft, has coded patterns of opaque and transparent sectors. As the disk rotates, these patterns interrupt the light emitted onto the photodetector, generating a digital or pulse signal output [27]. According the pattern of rotating disk, it can either be an absolute encoder or incremental encoder.

In this project, an incremental encoder HEDL 9140 is used and connected to the motor as position sensor. It has 500 counts per turn with 3 channels. The encoder readings are fed into motion control card PCI-7350, which provides quadrature decoding and converts both Channel A and B into 32-bits up/down counter values. Hence, the overall encoder gain in the system is $2000/2\pi$ counts per radian.

3. Amplifier

Figure 4-4: Amplifier B15A8

Amplifier is used to translate the low-energy reference signal from DAC into the high-energy power in term of voltage or current to run motor. The output torque generated by the motor is linearly proportional to the current supplied to it. In this project, the B15A8 amplifier is used. Some specification of the amplifier is shown in Table 4-3.

Peak Current	±15 A
Maximum Continuous Current	±7.5 A
Supply Voltage	20 – 80 V (DC)
Maximum allowable voltage supplied to amplifier	±10 V

Table 4-3: Specification of B15A8 amplifier

As the maximum current tolerable by the motor is 5.10 A, the maximum allowable current supplied by the amplifier is being tuned down to 5.10 A. This amplifier has two modes

- Voltage mode: input signal as well as output signal, they are voltage
- Current/torque mode: input signal is voltage and output signal is current

For the position control system, current mode amplifier is used to provide high stiffness to the system for positional accuracy and restricting movement from desired position.

Amplifier's adjustments are conducted in "switch functions" and "potentiometer functions"

Switch Function:

SWITCH	SETTING	FUNCTION DESCRIPTION
1	OFF	No effect of Duty-cycle feedback
2	ON	120 degree communication phase setting
3	ON	Shorts out the velocity/voltage loop integrator capacity
4	OFF	Offset

Table 4-4: Amplifier's Switch Function tuning

Potentiometer Functions:

-Pot1: Turn fully CCW in current mode

-Pot2: NA

-Pot3: Adjusting the ratio between input signal (voltage) and output signal (current)

Supply a 10V into pin 4 (+REF IN) (indicating the input signal to amplifier), turning this pot such as the signal at pin is 5.10A (corresponding to 2.6V in potential meter) (indicating the output signal from amplifier) that is the maximum continuous current motor can attain.

-Pot4: Adjusting any imbalance in the input signal or in the amplifier

Grounding both 2 pins 4 (+REF IN) and 5 (-REF OUT): (indicating no input signal to amplifier), turning this pot such as the signal at pin 8 (CURR MONITOR OUT) is 0 mA (indicating the output signal from amplifier)

4. Motion controller:

Figure 4-5: Motion controller card PCI-7350

The motion controller PCI-7350 as shown in the figure is the brain of the control system. It connects the user interface with the use of Labview and MAX and the rest of the system. PCI-7350 receives the command from Labview software as well as MAX, feedback from the incremental encoder to send the signal to DAC, then amplifier to run the motor. The PID controller integrated inside PCI-7350 help system to get smooth motion and correct desired position.

4.2.2. Software development:

A/ PID tuning:

When operating the motion, the controller continuously reads the position of the feedback device (encoder) and compares it to the current trajectory position (desired position). The purpose of PID controller is to make the smooth and fast response from the motor, to get the target position as soon as possible. To find out the PID gains for control loop, the report will present practical method as well as the theoretical method to find the optimal value for PID control loop.

A.1/ Practical adjustment:

Conducting the step response in Servo Tune of MAX as shown in the Figure4-6, setting the step length as 1000 counts and samples as 200

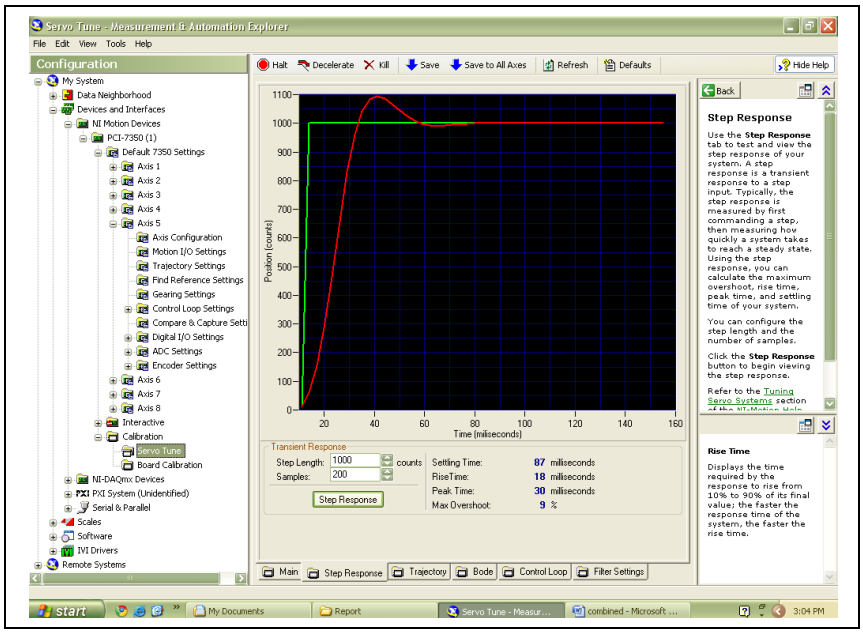

Figure 4-6: Step response in Servo Tune of MAX

1. Set all three PID parameters, K_P, K_D and K_I to be 0
2. Increasing the K_P value gradually, click the "Step Response" button to view a step response graph of current set PID value. If the graph shows the parameter
   - too low-double the value of the K_P
   - too high-set the parameter to be middle value of current value and the previous value

   Repeat step 2 until a reasonable value for K_P is achieved. This means the response will approach the desired position with continuing oscillation about input and small amount of damping as shown in figure 4.6

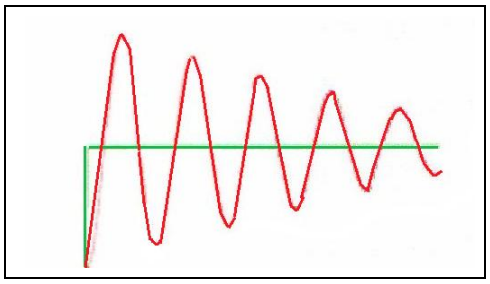

Figure 4-7: Oscillatory signal

3. Repeat step 2 for K_D value until the response will no longer oscillate, but quickly dampen to a steady state value

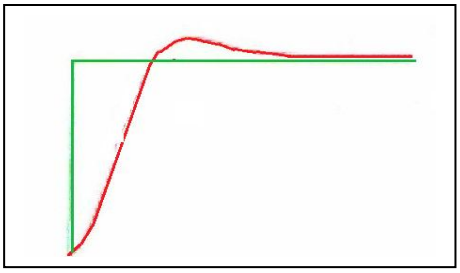

Figure 4-8: Steady state error

4. Repeat the step 2 for K_I value until the steady state value in step 3 is consistent as the input position

Finding value is K_P = 130 , K_D = 1200, K_I = 1

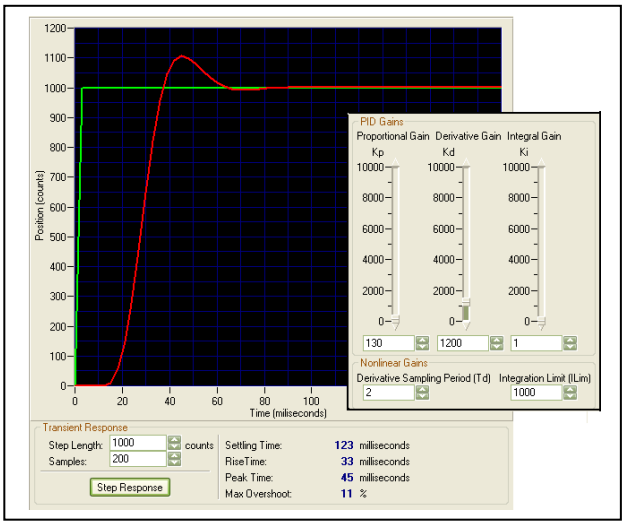

Figure 4-9: Step response with PID values from practical approach

A.2/ Theoretical approach:

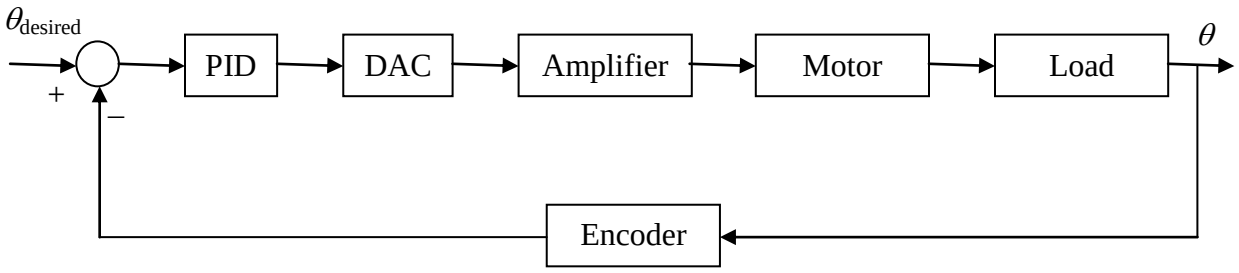

Figure 4-10: Transfer function of control system

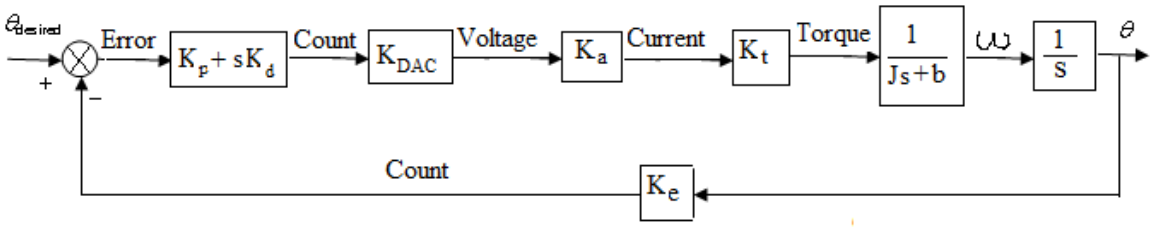

Figure 4-11: Mathematical model of transfer function

- K_P and K_D: proportional and derivative gains of PID

  Both gain values needed to find

- K_{DAC} : the gain of digital-to-analogue convertor

  In DAC, the range of output is ±10V, the input signal is 16bit-binary

  K_{DAC}=20V/2^16counts

- K_a : the gain of amplifier

  Maximum input voltage is 10V, maximum output current=max continuous current of motor=5.10A

  K_a=5.10A/10V

- K_t :torque constant of motor, from datasheet, K_t=37.1mNm/A

- 1/(Js+b): the transfer function from torque to shaft's angular velocity of motor

  J is rotor inertia =119gcm^2=1.19x10^{-5} kgm^2, the resulting motor model with viscous damping often b≈0 and can be neglected

- 1/s: the transfer function from shaft's angular velocity of motor to shaft's position
- K_e the transfer function of encoder, 1 revolution corresponds to 2000 counts

  K_e = 2000counts/2π

To make a desired response, two parameters are set such as: overshoot and settling time. Such values chosen for this response are shown in Table 4-5

	Settling time (t_s)	**% Overshoot (%M)**
Set 1	0.05	10
Set 2	0.06	5
Set 3	0.07	5

Table 4-5: Set of settling time and overshoot values for PID tuning

Selecting set 1 as an example for calculation.

The formula for overshoot and settling time:

%M = exp(-π*ζ/sqrt(1-ζ^2))

t_s = 4.6/(ζ*ω_n)

In which: ζ damping ratio, ω_n: natural frequency of system.

For set 1: M=0.1, t_S=0.05

0.1= exp(-π*ζ/sqrt(1-ζ^2)) so ζ=0.5914

0.05=4.6/(ζ*ω_n)= 4.6/(0.5914*ω_n) so ω_n=155.56

The desired closed-loop poles: $s = -\zeta\omega_n \pm j\omega_n\sqrt{1-\zeta^2}$

Similar conducting calculations for sets 2 and 3, the following table obtained:

	Desired closed-loop pole (s)
Set 1	$s_{1,2} = -92 \pm j125.4$
Set 2	$s_{1,2} = -76.7 \pm j82.1$
Set 3	$s_{1,2} = -65.71 \pm j70.37$

Table 4-6: Desired closed-loop poles

The models in transfer function of position control loop combine both z-domain (discrete signal) and s-domain (continuous signal):

- DAC is based on z-domain which the gain $D(z)=K_P+K_D(1-z^{-1})+K_I/(1-z^{-1})$ or $D(s) = k_P + sk_D + k_I/s$

  $K_P = k_p$; $K_D = k_D/T$; $K_I = T*k_I$ (T:sampling time)

- The rest based on s-domain

<u>Continuous approximation approach:</u>

All the models of the mixed s-domain and z-domain system are all converted to the s-domain. When the sampling time T is small, the effect of the zero order hold is neglected. (zero order hold is a mathematical model of the practical signal re-construction done by a conventional digital-to-analogue converter (DAC). That is, it describes the effect of converting a discrete-time signal to a continuous-time

signal by holding each sample value for one sample interval. It has several applications in electrical communication.)

The open-loop transfer function of system:

$$L_{(S)} = (k_P + k_D s) * K_{DAC} * K_a * K_t * \frac{1}{Js} * \frac{1}{s} * K_e$$

$$L_{(S)} = (\frac{k_P + sk_D}{s^2})154.53$$

Let

$$\omega_c \approx \omega_n \sqrt{(1-2\zeta^2) + \sqrt{4\zeta^4 - 4\zeta^2 + 2}} = 180.4$$

$$\gamma = \tan^{-1}\left[\frac{2\zeta}{\sqrt{-2\zeta^2 + \sqrt{1+4\zeta^4}}}\right] = 58.6^0$$

In any system: $|L(j\omega_c)|=1$ and $\angle L(j\omega_c) = \gamma - \pi$

$$\rightarrow L_{(j180.4)} = (\frac{k_P + j180.4k_D}{180.4^2})154.53$$

Let

$$r = \sqrt{k_P{}^2 + (180.4k_D)^2}$$

$$\theta = \tan^{-1}\left(\frac{180.4k_D}{k_P}\right)$$

$$\rightarrow L_{(j180.4)} = 4.75\times10^{-3} re^{j(\theta-\pi)}$$

$$|L_{(j180.4)}| = 4.75\times10^{-3} r = 1 \rightarrow r = 210.6$$

$$\angle L_{(j180.4)} = \theta - \pi = \gamma - \pi \rightarrow \theta = \gamma = 58.6^0$$

So the analogue PID controller given as k_D=0.996, k_P=109.72

With T=0.001s the digital PID controller: K_D=996 , K_P=109.72

Digital approach:

After a controller is designed using the continuous approximation method, it is important to perform a z-domain analysis since the final control scheme is eventually implemented on a microprocessor and it is desirable to see the effect of the designed D(s) controlling the system. The z-domain is to digital system what the s-domain is to continuous time system. We look at the poles and zeros on the z-plane in the same manner as we look for them in the s-plane. The main difference is that for stability, the closed loop poles must be inside the unit circle on the z-plane.

The only digital component in a motion control system is the controller. All other components after treated as continuous time.

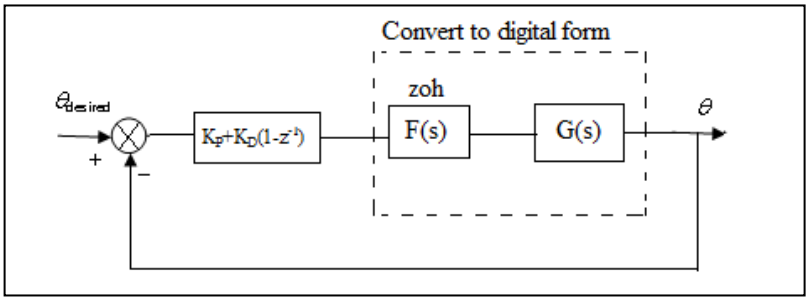

Figure 4-12: Control loop representation for position control

The zoh has a transfer function of the form: $F(s)=\frac{1-e^{-Ts}}{s}$

G(s) is the open loop of system without PID controller: $G_{(S)}=\frac{154.53}{s^2}$

Let

$$G_0(z)=Z\{F(s)G(s)\}=(1-z^{-1})Z\{\frac{G(s)}{s}\}=(1-z^{-1})Z\{\frac{154.53}{s^3}\}=\frac{154.53}{2}\left(\frac{T^2(z+1)}{(z-1)^2}\right)$$

The closed-loop transfer function of the system: $T(z)=\frac{D(z)G_0(z)}{1+D(z)G_0(z)}$

The characteristic equation given by:

$$1+D(z)G_0(z)=0$$
$$\rightarrow 1+\left(K_P+\frac{K_D(z-1)}{z}\right)\left\{\frac{154.53}{2}\left(\frac{T^2(z+1)}{(z-1)^2}\right)\right\}=0$$
$$\rightarrow 1+7.73\times10^{-5}\frac{\left(\{K_P+K_D\}z-K_D\right)(z+1)}{z(z-1)^2}=0$$

Let $A = K_p + K_D$ and $B = K_D/(K_P+K_D)$

$$\rightarrow 1+7.73\times10^{-5}\frac{\left(\{K_P+K_D\}z-K_D\right)(z+1)}{z(z-1)^2}=0$$

$$\rightarrow z(z-1)^2+7.73\times10^{-5}A(z-B)(z+1)=0 \qquad (*)$$

Using the pole-zero mapping: $z = e^{sT}$

$$\rightarrow z_{1,2} = e^{(-92\pm j125.4)(0.001)}$$

$\rightarrow z_{1,2} = 0.905 \pm j0.1141$ should be the roots of equation...

From equation (*):

$$\angle(z_1-B)+\angle(z_1+1)-\angle z_1-2\angle(z_1-1)=\pi$$

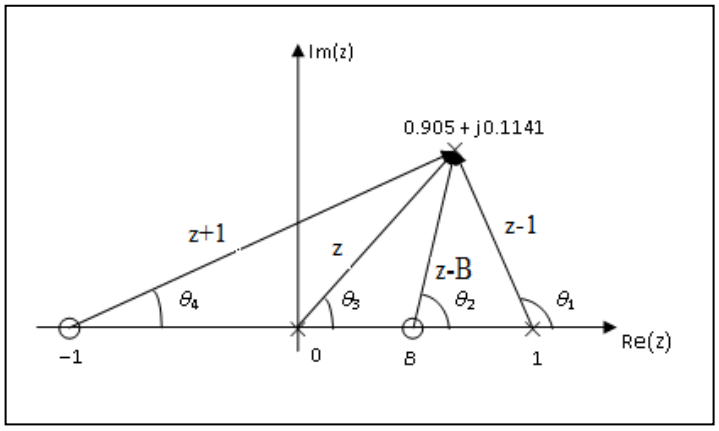

Figure 4-13: Closed-loop poles in Z-plane

$$\therefore \theta_2 + \theta_4 - \theta_3 - 2\theta_1 = \pi$$

$$\rightarrow \theta_2 + \tan^{-1}\left(\frac{0.1141}{0.905+1}\right) - \tan^{-1}\left(\frac{0.1141}{0.905}\right) - 2\left(\pi - \tan^{-1}\left(\frac{0.1141}{1-0.905}\right)\right) = \pi$$

$$\rightarrow \theta_2 = 1.46 rad$$

Because $\tan\theta_2 = 0.1141/(0.905 - B) \rightarrow B = 0.892$

Subs B=0.892 and z= 0.905+j0.1141 into (*)

$\rightarrow$ A=1,187

$\rightarrow K_D = 1058, K_P = 128$

With sets 2 and 3, the similar method is applied to find the digital as well as continuous approxiamtion. K_i = 1 is added to the PD controller to eliminate the steady-state error. The results are shown in the below tables:

Table 4.7: PID values from analysis methods.

	Digital	**Continuous Approximation**	**Selected PID values**
Set 1	K_p = 128 K_D = 1058 K_I = 1	K_p = 110 K_D = 996 K_I = 1	K_p = 128 K_D = 1058 K_I = 1
Set 2	K_p = 69 K_D = 885 K_I = 1	K_p = 38 K_D = 677 K_I = 1	K_p = 69 K_D = 885 K_I = 1
Set 3	K_p = 49 K_D = 722 K_I = 1	K_p = 28 K_D = 581 K_I = 1	K_p = 49 K_D = 722 K_I = 1

With analytical approach, $K_P = 128$, $K_D = 1058$, $K_I = 1$ (Set1)

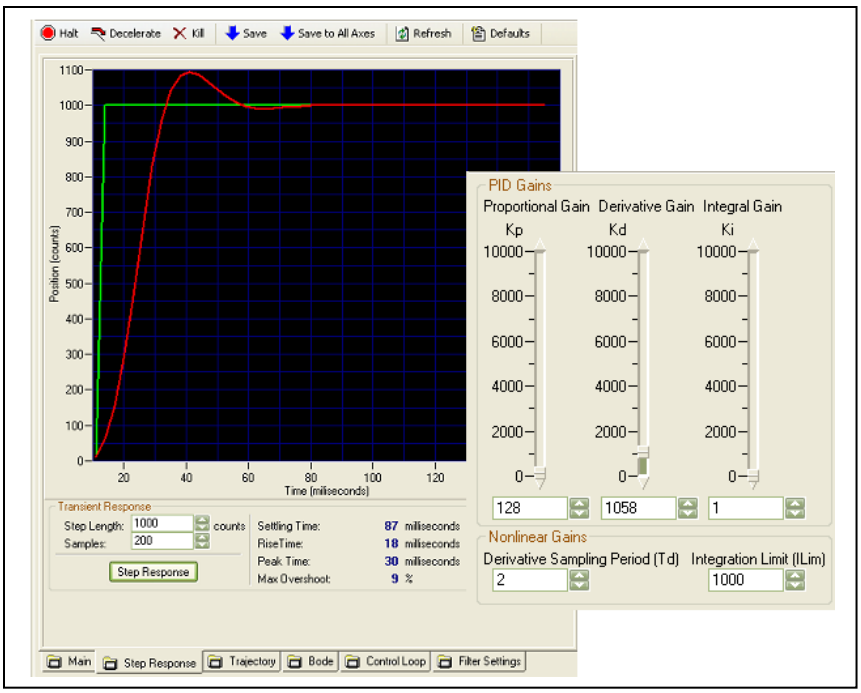

Figure 4-14: Step response with PID values from analytical approach

The response of PID value with set 1 has the overshoot which is about 10% (100counts) as the same value as we expected in calculation. It proves that the analytical approach is quite accurate in finding the range of PID parameter for control system.

Comparing the responses between the practical approach (Figure 4-9) and analytical approach (Figure 4-14), they are approximately the same. The analytical values are chosen for handling the motion of motor.

B/ Labview program:

B.1. Algorithm for motion of motors:

The purpose of program is to make sure that for one movement, all the motors that pull the cables in one module should operate simutaneously (start and finish the rotation at the same time). To achieve this purpose, the trapezoidal move profile of motor will hepls us to find the best way to do the program.

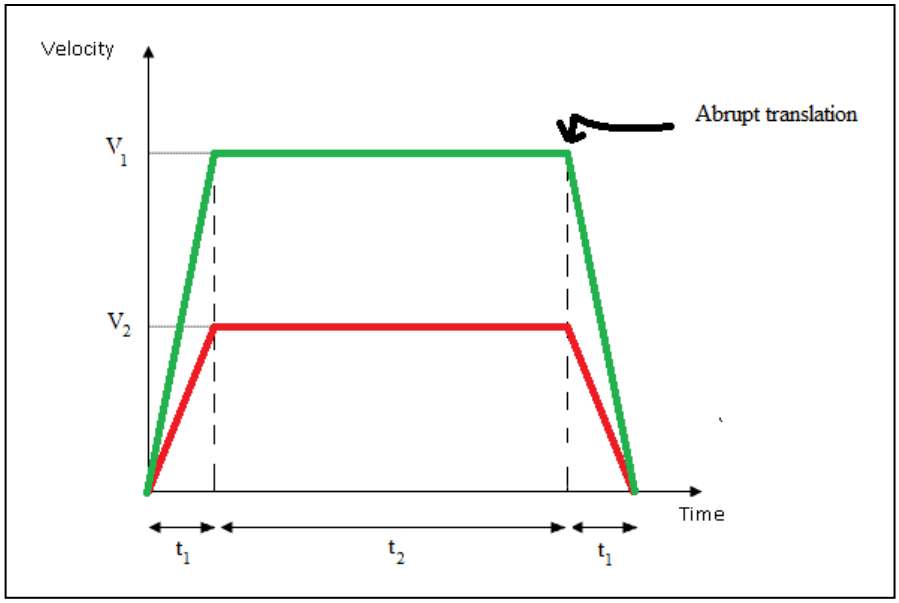

Figure 4-15: Velocity profile of any 2 motors

Considering the velocity profile of two motor as shown in the firgure. The red and green color respectively represent the linear velocity profiles of motor 2 and 1(will be proportional to the angular velocity of motor). assuming both motors accelerate and decelerate in the same duration t_1, motor 1 will achieve velocity V_1 after accelerating, while motor 2 achieves V_2. As foundation of physics, the area under velocity profile represents the displacement that corresponding to the change in cable length.

Deta L_1= D_1=V_1*(t_1+t_2)

Deta L_2= D_2=V_2*(t_1+t_2)

So $\frac{\triangle L_1}{\triangle L_2} = \frac{V_1}{V_2}$

Moreover, to make sure that both motors will accelerate and decelerate in the same duration t_1 so $\frac{A_1}{A_2} = \frac{V_1 / t_1}{V_2 / t_1} = \frac{\triangle L_1}{\triangle L_2}$

To sum up, the conditions in program to make both motor operate simutaneously is:

$$\frac{A_1}{A_2} = \frac{V_1}{V_2} = \frac{\triangle L_1}{\triangle L_2}$$

However, the acceleration as well as deceleration should be smooth rather than abrupt transition, so the jerk value=100counts/s^3 is added into the motion profile.

B.2. Main parts in program

a. R matrix:

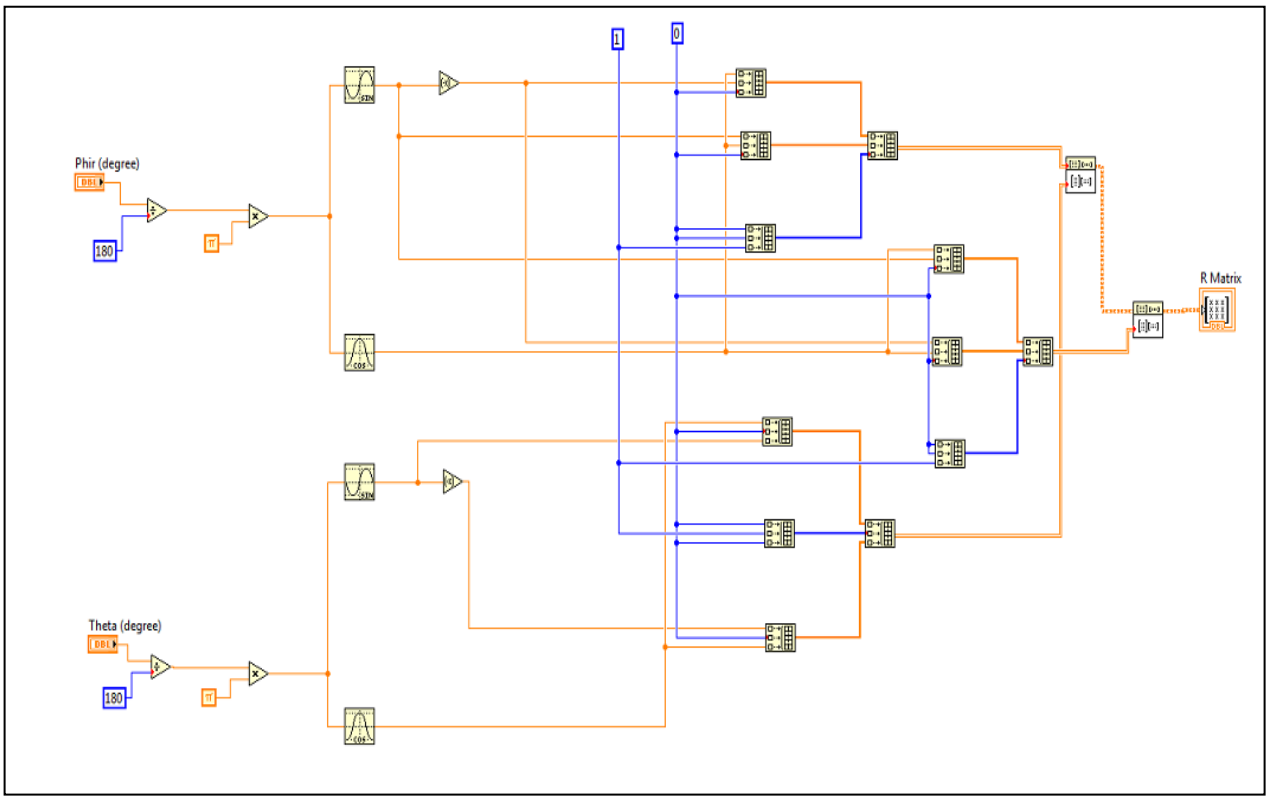

Figure 4-16: The R-matrix subIV-Labview program

The function of this subIV is to create R matrix that will be used in kinematic analysis process to find the cable length at instance of time. The input data is theta and phi angles, the output is the R matrix as represented in section 1 of chapter 3.

b. Finding the cable length:

To demonstrate the algorithm of program, one subIV: finding the cable length 1 is used to represent. From chapter 3: the length of cable 1 is based on the modulus of vector:

$$Vector1 = \begin{pmatrix} -r \\ 0 \\ 0 \end{pmatrix} + \begin{pmatrix} 0 \\ 0 \\ L_1 \end{pmatrix} + R_{(\phi_1;\theta_1)} \begin{pmatrix} 0 \\ 0 \\ L_1 \end{pmatrix} + R_{(\phi_1;\theta_1)} \begin{pmatrix} r \\ 0 \\ 0 \end{pmatrix}$$

In which: R(Φ,Θ) is R matrix as stated in previous section . L_1 is new length of imaging universal joint module, calculating based on the formula:

$$L = \frac{2L_0}{\theta} \tan\left(\frac{\theta}{2}\right) \qquad (**)$$

Note that, if theta=0, the L_1 remains the same as initial backbone length L_0, the formula (**) is invalid. As that reason, the case structure is used.

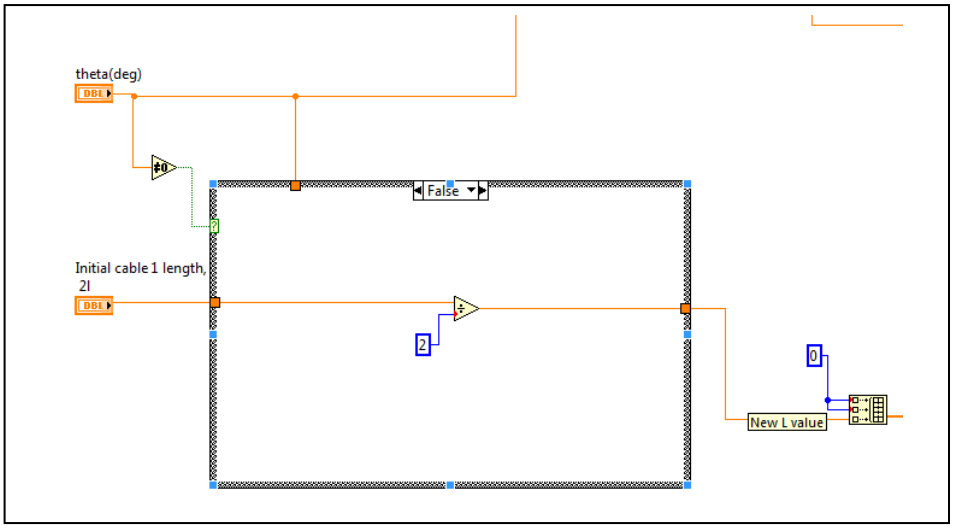

Figure 4-17: "False case" for new length of imaging universal joint module calculation

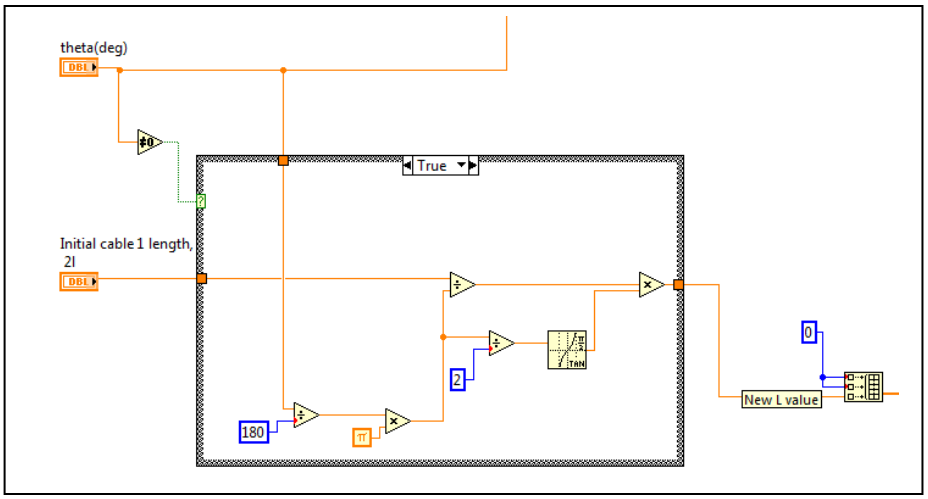

Figure 4-18: "True case" for new length of imaging universal joint module calculation

In the program, each vector term in the formula is created. The R-matrix subIV also used helps to create 2 last terms of formula. After all vectors are created, they will be summed up and take modulus to find the instant cable length.

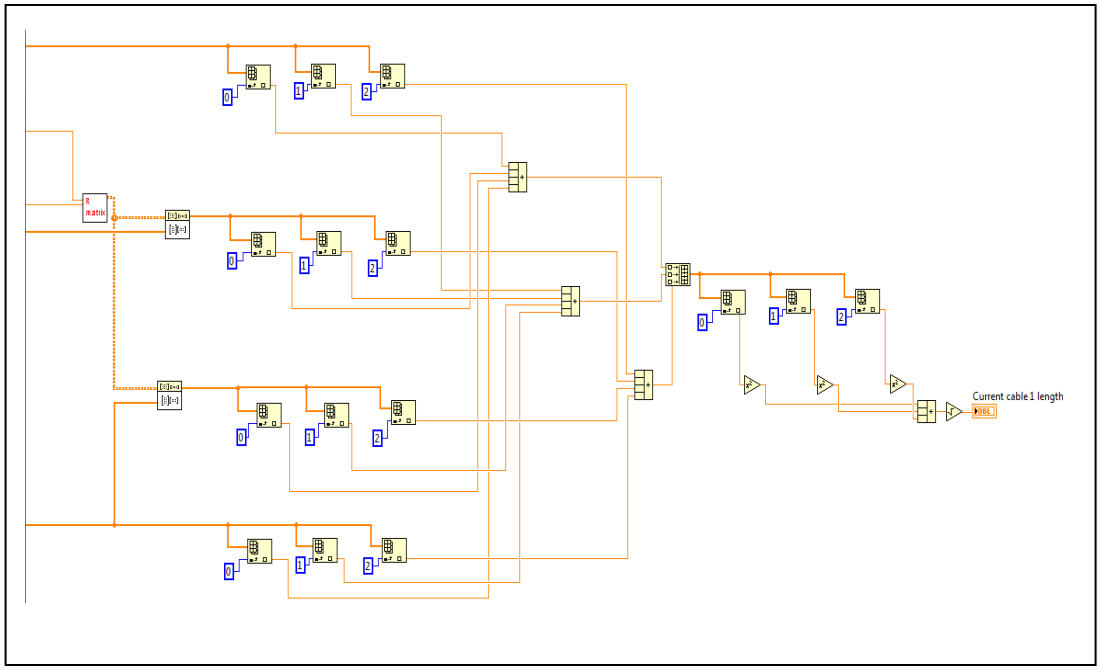

Figure 4-19: Portion of Labview program to find the cable length

c. Velocity and acceleration loading:

When the instant cable length is determined, based on the previous cable length, the program calculates the change in length as the displacement motor should make by rotating. After the changes in length of all cables evaluated, the velocity and acceleration are loading to motor is equal to the ratio between each cable length change and maximum change multiplies the maximum velocity and maximum acceleration that motor can suffer. This loading value will satisfy the condition:

$$\frac{A_1}{A_2} = \frac{V_1}{V_2} = \frac{\triangle L_1}{\triangle L_2}$$

and all motor will operate simultaneously.

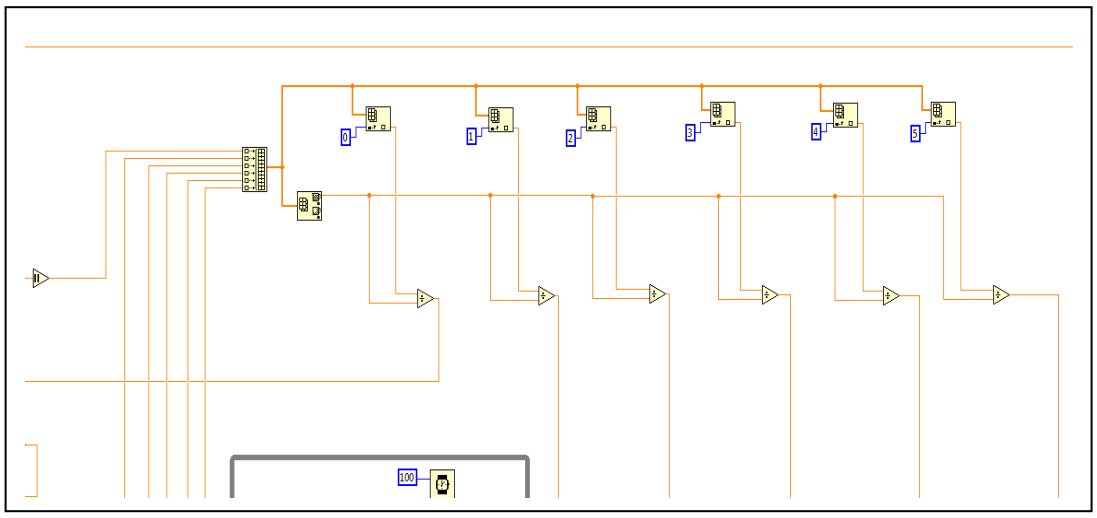

Figure 4-20: Portion of the Labview programme which ensures all motors stop together in one step

d. Running motor:

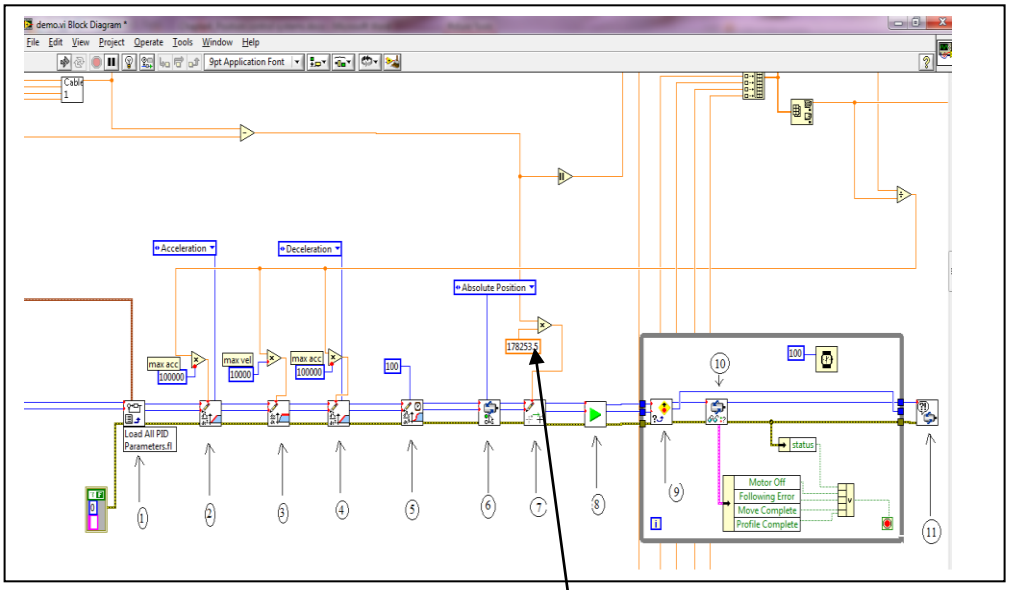

Figure 4-21: Portion of the Labview programme which runs the motor

1.	Load PID value	7.	Load target position in counts
2.	Load acceleration	8.	Start motion
3.	Load velocity	9.	Check move complete status
4.	Load deceleration	10.	Read per axis status
5.	Load jerk	11.	Motion Error handler
6.	Set operation mode		

CHAPTER 5: EXPERIMENT AND RESULTS

5.1. **Objectives:**

- Evaluating the accuracy of kinematic analysis
- Evaluating the method to control the endpoint position of cable-driven robotic arm
- Investigating the accuracy of position control in cable-driven robotic arm, hence to apply the robotic arm in necessary field of industry

5.2. **Equipments:**

1. **Conducting the movement of robotic arm's modules:**
    - All the devices stated in hardware setup including:
        - Actuation unit: Brushless DC servomotor, Gearbox and belt-chain reduction system
        - Incremental Encoder
        - Amplifier B15A8
        - UMI-7764 connection box
        - Motion controller card PCI-7350
        - DC 24V source (supply for motor) and 5V source (supply for encoder and amplifier)
        - Computer with labview software
    - Physical construction of one module

- Holder design to hold the backbone
- Cable: Clear nylon coated stainless steel fishing wire (150LB or 68kg test)
- Backbone: length($2L_0$) =120mm, diameter = 6mm, material: Delrin

2. **Testing the accuracy of movement:**
    - Using the compact and ruler to measure the cable lengths and backbone distance
    - Microsoft office (Excel) to record all the data and plot the graphs

5.3. **Procedures:**

For accuracy of position control motion, the experiment in this project is conducted with one module

- ❖ Checking the status all the hardware setup including: the adjustment of amplifier, PID tuning parameter, connection and power supplies
- ❖ Initializing the module 1 vertical direction in which each cable length is equal to the backbone length. It is important to make sure that all the cables are in pre-tension before the movement. To attain this situation, using MAX, to set some desired position for motor until the cables are in tension.
- ❖ Input the value r = 50mm (radius of module's base) and initial backbone's length $2L_0$ = 120mm into the labview program

The experiment is conducted with 12 sets of theta and phi values, the practical and theoretical value of cable length 1, 2, 3 as well as the distance between endpoint and global coordinate's origin (called as backbone distance, shown in Figure 5-1) are:

	Set 1	**Set 2**	**Set 3**	**Set 4**	**Set 5**	**Set 6**	**Set 7**	**Set 8**	**Set 9**	**Set 10**	**Set 11**	**Set 12**
Theta 1(<60^0)	30^0	30^0	30^0	40^0	40^0	40^0	50^0	50^0	50^0	60^0	60^0	60^0
Phi 1(<36^0)	5^0	15^0	25^0	5^0	15^0	25^0	5^0	15^0	25^0	5^0	15^0	25^0

Table 5-1: Sets of theta and phi angles for experiment

- For practical values of distances: Using the compact and ruler to measure the cable lengths and backbone distance
- For theoretical values of distances: the values are shown in the front view of labview program. Recording those values.

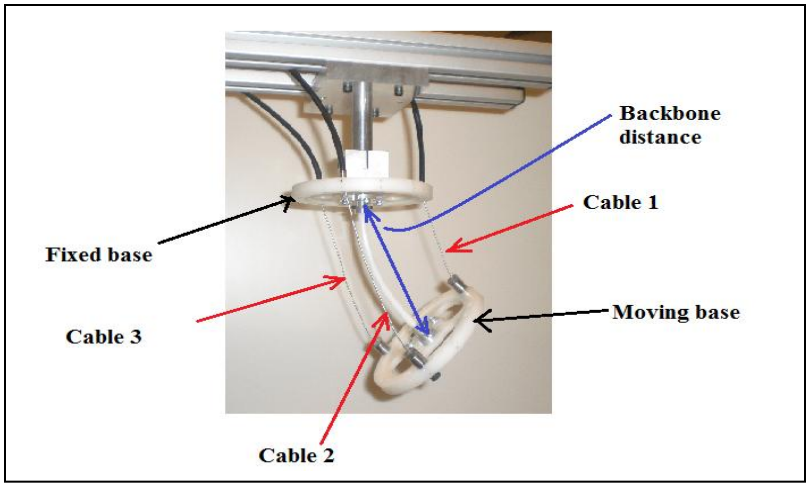

Figure 5-1: Feature of robotic arm with one module

5.4. **Results:**

1. Backbone Distance:

	Set 1	Set 2	Set 3	Set 4	Set 5	Set 6	Set 7	Set 8	Set 9	Set 10	Set 11	Set 12
Theoretical value(mm)	118.634	118.634	118.634	117.578	117.578	117.578	116.228	116.228	116.228	114.592	114.592	114.592
Practical value(mm)	119	119	118.5	117	116	117	116	115	116.5	113	112.5	112
Error (%)	-0.31	-0.31	0.11	0.49	1.34	0.49	0.20	1.06	-0.23	1.39	1.83	2.26

Table 5-2: Theoretical and practical values for backbone distance

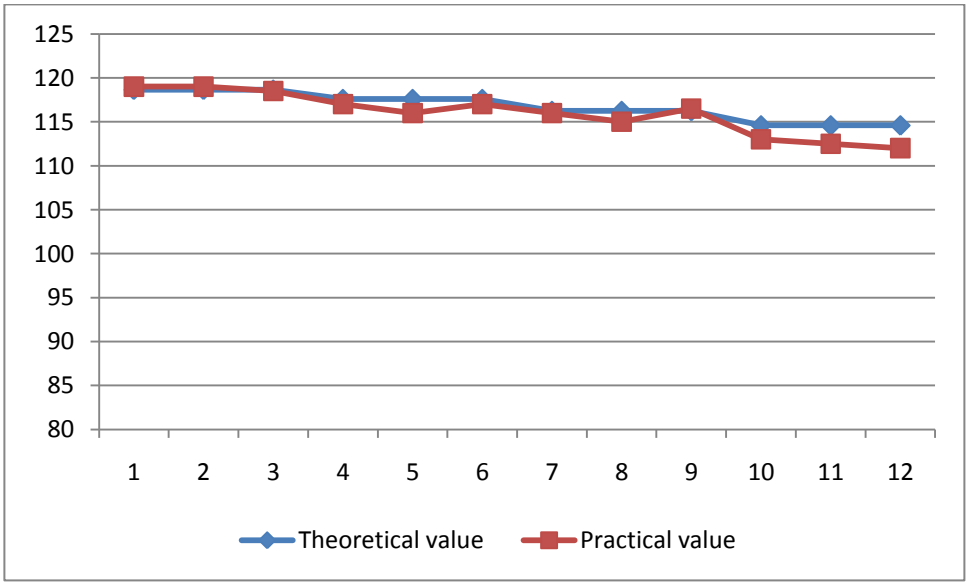

Graph 5-1: Theoretical and practical values for backbone distance

$$\text{Maximum error} = \frac{114.592 - 122}{114.592} = 2.26\% \text{ (set 12)}$$

$$\text{Minimum error} = \frac{118.634 - 118.5}{118.634} = 0.11\% \text{ (set 3)}$$

2. Cable 1 ‘s length:

	Set 1	Set 2	Set 3	Set 4	Set 5	Set 6	Set 7	Set 8	Set 9	Set 10	Set 11	Set 12
Theoretical value(mm)	92.8505	93.6339	95.1769	83.506	84.5413	86.5803	74.1274	75.4066	77.9261	64.7818	66.2953	69.2762
Practical value(mm)	99	99	99.5	84	88.5	90.5	77.5	79.5	80.5	66	66	73
Error (%)	-6.62	-5.73	-4.54	-0.59	-4.68	-4.53	-4.55	-5.43	-3.30	-1.88	0.45	-5.38

Table 5-3: Theoretical and practical values for cable1’s length

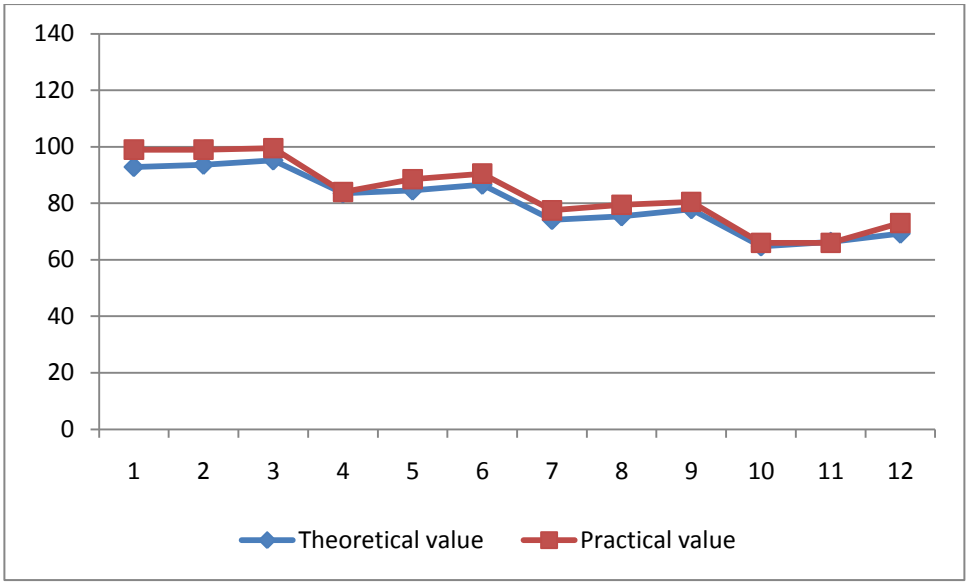

Graph 5-2: Theoretical and practical values for cable1’s length

$$\text{Maximum error} = \frac{92.8505 - 99}{92.8505} = -6.62\% \text{ (sets 1)}$$

$$\text{Minimum error} = \frac{66.2953 - 66}{66.2953} = 0.45\% \text{ (set 11)}$$

Cable 2's length:

	Set 1	Set 2	Set 3	Set 4	Set 5	Set 6	Set 7	Set 8	Set 9	Set 10	Set 11	Set 12
Theoretical value(mm)	129.572	125.333	120.89	132.032	126.43	120.559	134.089	127.167	119.912	135.722	127.533	118.949
Practical value(mm)	128.5	126	122	130.5	126.5	123	133	130.5	122	136.5	131	127
Error (%)	0.83	-0.53	-0.92	1.16	-0.06	-2.02	0.81	-2.62	-1.74	-0.57	-2.72	-6.77

Table 5-4: Theoretical and practical values for cable2's length

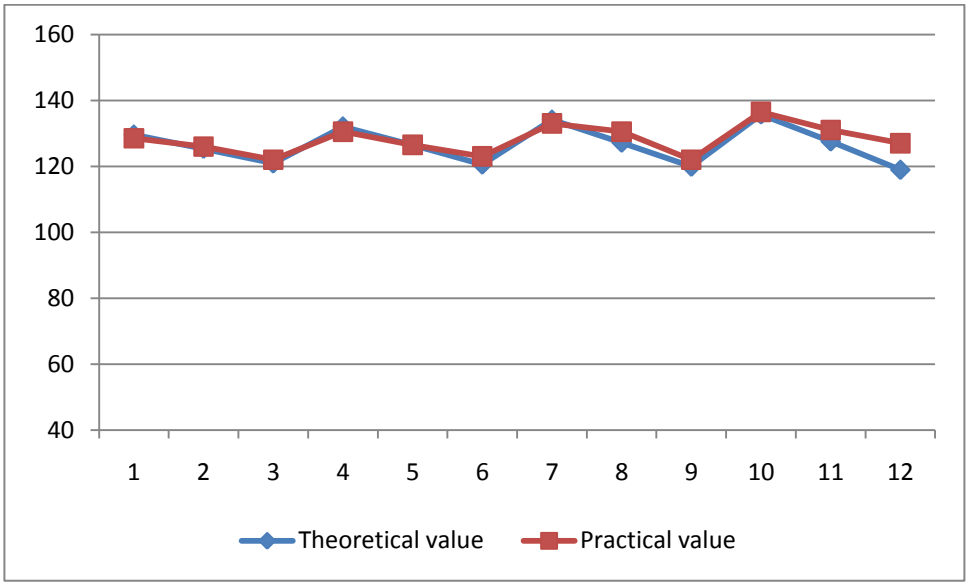

Table 5-3: Theoretical and practical values for cable2's length

$$\text{Maximum error} = \frac{118.949 - 127}{118.949} = -6.77\% \text{ (set 12)}$$

$$\text{Minimum error} = \frac{125.333 - 126}{125.333} = -0.53\% \text{ (set 2)}$$

3. Cable 3's length:

	Set 1	Set 2	Set 3	Set 4	Set 5	Set 6	Set 7	Set 8	Set 9	Set 10	Set 11	Set 12
Theoretical value(mm)	133.479	136.935	139.835	137.195	141.762	145.595	140.469	146.112	150.847	143.27	149.947	155.549
Practical value(mm)	133	135	136	135.5	140	141	137	144.5	147	144	146	147
Error (%)	0.36	1.41	2.74	1.24	1.24	3.16	2.47	1.10	2.55	-0.51	2.63	5.50

Table 5-5: Theoretical and practical values for cable3's length

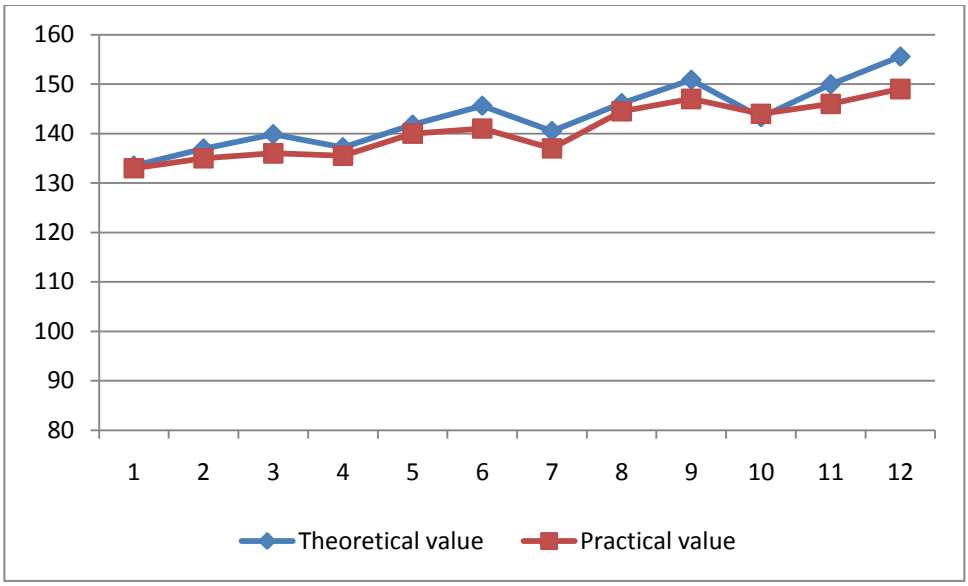

Graph 5-4: Theoretical and practical values for cable3's length

$$\text{Maximum error} = \frac{155.549 - 147}{155.549} = 5.50\% \text{ (set 3)}$$

$$\text{Minimum error} = \frac{133.479 - 133}{133.479} = 0.36\% \text{ (set 12)}$$

5.5. **Discussion:**

1. Backbone distance:

First of all, the backbone distance represents the distance between centre points of two base for first module. Because it is difficult to represent the endpoint vector in frame 10 (global coordinate), in this experiment, to test the accuracy in movement of 1 module, only the distance from endpoint to origin of frame 10 is determined. From graph 5.1, the difference between theoretical values and practical values are approximately the same. The difference is smaller than 2.26%, this proves that in the kinematic analysis, the following assumptions are approximately correct:

- The length of backbone remains the same during the bending
- The configuration of 1 module can be assumed as the configuration of universal joint as stated in chapter 3.

2. Cable lengths:

With 3 graphs 5-2. 5-3 and 5-4, the practical values follow the theoretical values with the same trends. Those changing can be observed clearly from graphs are

- Cable length 1: when the theta value increases, the cable length will decrease
- Cable length 2: when the phi value increases, the cable length will decrease
- Cable length 3: when the phi value increases, the cable length will increase

The results that were obtained from the practical approach are approximately the same as the theoretical values that are based on the kinematic analysis. The max-

imum different in the cable lengths is only around 4-5 mm. This error may come from the mechanical system and measurement such as:

- The minimum scale of rule is only 1mm
- The cable cannot wrap drum in actuation unit properly.

These issues are difficult to avoid in the practical approach. To sum up, the experiment proves that, the kinematic analysis is correct and it can be used for future applications.

CHAPTER 6: CONCLUSION AND FUTURE WORK

6.1. Conclusion:

The aim of the project was to design and implement the motion control on a cable-driven dexterous robotic arm prototype using the software platform Labview. The study focused on the implementation of position control of 2-module cable-driven dexterous robotic arm. The method is based on the kinematic and inverse kinematic of mechanism using Euler orientation representation. With PID controller connected with amplifier as well as motor through UMI box connection, the commands from labview program will make the motor's operations. The PID parameters help managing the optimal motion of motor without big delay. These values could be determined by analytical or practical methods. According to experiment results, it was found that with the cable-driven robotic arm can be controlled easily. Using the motor for control the cable length, the target position is clearly obtained. All motors operated simultaneously to give the smooth movement for robotic arm. However, there are some limitations of this project. If the end-effector coordinate can be determined, it would give a better conclusion about the accuracy of position control for this system. From this project, we infer that the cable-driven robotic arm can work well in many fields such as: industry, security and defence (search and rescue) that require high speed operation with high accuracy, deal in constrained workspace and some replaces the appearance of human. Therefore, the developing in dexterous robotic arm using CDPM is very significant and important nowadays.

6.2. Future Works:

In future, other experiment should be conducted to evaluate the accuracy in position control with 2, 3, 4 modules and so on. The different geometry of backbone also could be conducted to find the best geometry for controlling motion of robotic arm.

Finding the optimal way to determine the accuracy in position control

It is very common to implement force control with position control on cable-driven mechanism as this can ensures that the robotic arm has enough mechanical power to carry its load.

Besides, the velocity control is also one important aspect that is needed to investigate.

REFERENCES

[1]: P. Gholami, M. Aref, H.Taghurad., "On the Control of the KNTU CDRPM: A Cable Driven Redundant Parallel Manipulator", *2008 IEEE/RSJ International Conference on Intelligent Robots and Systems*, Sept.2008.

[2]: RL. Williams, P. Gallina, J. Vadia., "Planar Translational Cable-Direct Driven Robots", *Journal of Robotic Systems*, Vol. 20, No 3, pp.107-120, 2003.

[3]: "Snaking around in a nuclear jungle", Rob Buckingham and Andrew Graham, Int. J. Industrial Robot, Vol. 32, No. 2, ISSN 0143-991X, 2005, p120-127.[Online]. Available: http://www.ocrobotics.com/newsroom/publications/IR2005.pdf. [Accessed: July 10th 2010].

[4]: "Snake-arm robots slither forward", Jonathon Fildes, BBC News Website (bbc.co.uk), 13 September 2006. [Online]. Available: http://news.bbc.co.uk/2/hi/technology/5324708.stm. [Accessed: July 10th 2010].

[5]: Albus, J., Bostelman, R., and Dagalakis, N., "The NIST RoboCrane," *Journal of Research of National Institute of Standards and Technology*, Vol.97, May-Jun. 1992.

[6]: L.W. Tsai, *Robot Analysis – The mechanics of Serial and Parallel Manipulators*, A Wiley-Interscience Publication,1999.

[7]: J.P. Merlet, *Parallel Robots*, Kluwer Academic Publishers, 2000.

[8]: C.B. Pham, S.H. Yeo, and G.L. Yang, "Workspace analysis and optimal design of cable-driven planar parallel manipulators", in *Proceedings of IEEE Conference on Robotics, Automation and Mechatronics*, Singapore, December 1–3 2004, pp. 219–224.

[9]: S. Sahin and L. Notash, "Kinematics, workspace and stiffness analysis of wire-actuated parallel manipulators", in *Proceedings of World Congress in Mechanism and Machine Science*, Tianjin, China, April 01–04 2004, pp. 1868–1872.

[10]: A.B. Alp and S.K. Agrawal, "Cable suspended robots: Design, planning and control", in *Proceedings of IEEE Conference on Robotics and Automation*, Washington, DC., May 2002, pp. 4275–4280.

[11]: R.L. Williams II and P. Gallina, "Planar cable-direct-driven robots, part ii: Dynamics and control", in *Proceedings of the 2001 ASME Design Technical Conferences, Pittsburgh*, PA, September 9–12 2001.

[12]: C.B. Pham, S.H. Yeo, and G.L. Yang, "Tension analysis of cable-driven parallel mechanisms" in *Processing of IEEE Conference on Intelligent Robots and Systems*, Singapore, 2005, pp. 257-262.

[13]: A. Ming and T. Higuchi, "Study on multiple degree-of-freedom positioning mechanism using wires (part 2) – development of a planar completely restrained positioning mechanism", *International Journal of Japan Social Engineering*, vol. 28(3), pp. 235–242, 1994.

[14]: S. Masood. "Modelling and Control of Cable-Driven Robots," M.E.Thesis, Nanyang Technological University, Singapore, 2007.

[15]: Y.Yi, JE Mclnroy and Y Chen, "Over-constrained Rigid Multi Body Systems: Differential Kinematics, and Fault Tolerance," *Proceedings of Smart Structures and Materials 2002: Smart Structures and Integrated Systems*, Vol. 4701, pp. 189-199, Jul. 2002.

[16]: "Panasonic Professional Video Products – News and Events", Panasonic Professional Video Products. [Online]. Available: http://www.panasonic.com/business/provideo/news/images/snf_Skycam1.jpg. [Accessed: July 10th, 2010].

[17]: P. Gholami, M. Aref and H.Taghurad., "On the Control of the KNTU CDRPM: A Cable Driven Redundant Parallel Manipulator," *2008 IEEE/RSJ International Conference on Intelligent Robots and Systems*, Sept. 2008.

[18]: "PID controller", [Online]. Available: http://en.wikipedia.org/wiki/PID_controller. [Accessed: July 10th, 2010].

[19] "Understanding Servo Tune", NI Developer Zone. [Online]. Available: http://zone.ni.com/devzone/cda/tut/p/id/2923. [Accessed: July 10th, 2010].

[20]: Gravagne I.A., "Asymptotic regulation of a one-section continuum manipulator". in *IEEE/RSJ International Conference on Intelligent Robots and Systems*, Las Vegas, Nevada, Vol. 3, pp. 2779-2784, 2003.

[21]: Yamakita M., Hashimoto M. and Yamada T, "Control of locomotion and head configuration of 3D snake robot (SMA)", in *IEEE International Conference of Robotics and Automation*, Taipei, Taiwan, Vol. 2, pp. 2055-2060, 2003.

[22]: Matsuno F. and Suenaga K. (2002) *Control of redundant snake robot based on kinematic model.* SICE, Osaka, Japan, pp. 1481-1486.

[23] "Dextrous robot arm", ESA Automation & Robotics. [Online]. Available: http://www.esa.int/TEC/Robotics/SEM1IRNSP3F_0.html. [Accessed: July 10th 2010].

[24] "Snake-arm robots slither forward", By Jonathan Flides, Science and Technology reporter, BBC News. [Online]. Available: http://news.bbc.co.uk/2/hi/technology/5324708.stm. [Accessed: July 10th 2010].

[25]: Yamakita M., Hashimoto M. and Yamada T. (2003) *Control of locomotion and head configuration of 3D snake robot (SMA).* IEEE International Conference of Robotics and Automation, Taipei, Taiwan, pp. 2055-2060.

[26]: Bonev I.A. and Ryu J., "Orientation workspace analysis of 6-dof parallel manipulators", *ASME Design Engineering Technical Conferences*, Las Vegas, Nevada, pp. 1-8, 1999.

[27]: "Optical Encoder Fundamentals", NI Developer Zone, NI Website. [Online]. Available: http://zone.ni.com/devzone/cda/tut/p/id/4672. [Accessed: July 10th, 2010].

[28]:" Snake-like robot in search and rescue". [Online]. Available: http://dart2.arc.nasa.gov/Exercises/TMR2004/TMR-d2/images/23DSC00207.jpg. [Accessed: July 10th, 2010].

Appendix A:

Advanced Motion Control

Amplifier

Description

The B15A8 PWM servo drive is designed to drive brushless DC motors at a high switching frequency. A single red/green LED indicates operating status. The drive is fully protected against over-voltage, under voltage, over-current, over-heating and short-circuits across motor, ground and power leads. Furthermore, the drive can interface with digital controllers or be used stand-alone, and requires only a single unregulated DC power supply. Loop gain, current limit, input gain and offset can be adjusted using 14-turn potentiometers. The offset adjusting potentiometer can also be used as an on-board input signal for testing purposes.

Power Range

Peak Current	15 A
Continuous Current	7.5 A
Supply Voltage	20 - 80 VDC

Features

- Four Quadrant Regenerative Operation
- DIP Switch Selectable Modes
- Adjustable Current Limits
- High Switching Frequency
- Differential Input Command
- Digital Fault Output Monitor
- On-Board Test Potentiometer
- Offset Adjustment Potentiometer
- Adjustable Input Gain
- Selectable 120/60 Hall Commutation Phasing
- Drive Status LED
- Current Monitor Output

MODES OF OPERATION
- Current
- Open Loop
- Tachometer Velocity

COMMAND SOURCE
- ±10 V Analog

FEEDBACK SUPPORTED
- Halls
- Tachometer

COMPLIANCES & AGENCY APPROVALS
- UL
- cUL
- CE Class A (LVD)
- CE Class A (EMC)
- RoHS

SPECIFICATIONS

Power Specifications		
Description	Units	Value
DC Supply Voltage Range	VDC	20 - 80
DC Bus Over Voltage Limit	VDC	86
Maximum Peak Output Current[1]	A	15
Maximum Continuous Output Current	A	7.5
Maximum Power Dissipation at Continuous Current	W	30
Minimum Load Inductance (Line-To-Line)[2]	µH	200
Switching Frequency	kHz	33

Control Specifications		
Description	Units	Value
Command Sources	-	±10 V Analog
Feedback Supported	-	Halls, Tachometer
Commutation Methods	-	Trapezoidal
Modes of Operation	-	Current, Open Loop, Tachometer Velocity
Motors Supported	-	Brushed, Brushless, Voice Coil
Hardware Protection	-	Invalid Commutation Feedback, Over Current, Over Temperature, Over Voltage, Short Circuit (Phase-Phase & Phase-Ground)

Mechanical Specifications		
Description	Units	Value
Agency Approvals	-	CE Class A (EMC), CE Class A (LVD), cUL, RoHS, UL
Size (H x W x D)	mm (in)	129.3 x 75.8 x 25.1 (5.1 x 3 x 1)
Weight	g (oz)	280 (9.9)
Heatsink (Base) Temperature Range[3]	°C (°F)	0 - 65 (32 - 149)
Storage Temperature Range	°C (°F)	-40 - 85 (-40 - 185)
Form Factor	-	Stand Alone
P1 Connector	-	16-pin, 2.54 mm spaced, friction lock header
P2 Connector	-	5-port, 5.08 mm spaced, screw terminal

Notes

1. Maximum duration of peak current is ~2 seconds.
2. Lower inductance is acceptable for bus voltages well below maximum. Use external inductance to meet requirements.
3. Additional cooling and/or heatsink may be required to achieve rated performance.

PIN FUNCTIONS

P1 - Signal Connector			
Pin	Name	Description / Notes	I/O
1	+10V 3mA OUT	±10 V @ 3 mA low power supply for customer use. Short circuit protected. Reference ground common with signal ground.	O
2	SIGNAL GND		GND
3	-10V 3mA OUT		O
4	+REF IN	Differential Reference Input (±10 V Operating Range, ±15 V Maximum Input)	I
5	-REF IN		I
6	-TACH IN	Negative Tachometer Input (Maximum ±60 V). Use signal ground for positive input.	I
7	+TACH / GND	Positive Tachometer Input and Signal Ground	GND
8	CURRENT MONITOR	Current Monitor. Analog output signal proportional to the actual current output. Scaling is 2 A/V. Measure relative to signal ground.	O
9	$\overline{\text{INHIBIT IN}}$	TTL level (+5 V) inhibit/enable input. Leave open to enable drive. Pull to ground to inhibit drive. Inhibit turns off all power devices.	I
10	+V HALL 30mA OUT	Low Power Supply For Hall Sensors (+6 V @ 30 mA). Referenced to signal ground. Short circuit protected.	O
11	GND	Signal Ground	GND
12	HALL 1	Single-ended Hall/Commutation Sensor Inputs (+5 V logic level)	I
13	HALL 2		I
14	HALL 3		I
15	CURR REF OUT	Measures the command signal to the internal current-loop. This pin has a maximum output of ±7.25 V when the drive outputs maximum peak current. Measure relative to signal ground.	O
16	FAULT OUT	TTL level (+5 V) output becomes high when power devices are disabled due to at least one of the following conditions: inhibit, invalid Hall state, output short circuit, over voltage, over temperature, power-up reset.	O

P2 - Power Connector			
Pin	Name	Description / Notes	I/O
1	MOTOR A	Motor Phase A	O
2	MOTOR B	Motor Phase B	O
3	MOTOR C	Motor Phase C	O
4	POWER GND	Power Ground (Common With Signal Ground)	GND
5	HIGH VOLTAGE	DC Power Input	I

HARDWARE SETTINGS

Switch Functions

Switch	Description	Setting	
		On	Off
1	Open-loop mode selector. Activates internal PWM feedback.	Open-loop mode	Other modes
2	60/120 degree commutation phasing setting	120 degrees	60 degrees
3	Outer loop integration. Activates or deactivates integration. ON, by default, for current mode and OFF for other modes.	Inactive	Active
4	Test/Offset. Switches the function of the Test/Offset pot between an on-board command input for testing or a command offset adjustment. OFF by default.	Test	Offset

Mode Selection Table

	SW1	SW3	Tachometer
CURRENT	OFF	ON	Not Connected
OPEN LOOP	ON	OFF	Not Connected
TACHOMETER VELOCITY	OFF	OFF	Connected

Potentiometer Functions

Potentiometer	Description	Turning CW
1	Loop gain adjustment for open loop / velocity modes. Turn this pot fully CCW in current mode.	Increases gain
2	Current limit. It adjusts both continuous and peak current limit while maintaining their ratio.	Increases limit
3	Reference gain. Adjusts the ratio between input signal and output variables (voltage, current, or velocity).	Increases gain
4	Offset / Test. Used to adjust any imbalance in the input signal or in the amplifier. Can also be used as an on-board signal source for testing purposes.	Adjusts offset in negative direction

Note: Potentiometers are approximately linear and have 12 active turns with 1 inactive turn on each end.

Through-hole Components†

Location	Description
C8*	Velocity Loop Integrator. Through-hole capacitor that can be added for more precise velocity loop tuning. See section below on Tuning with Through-hole components for more details.
R158*	Tachometer Input Scaling. Through-hole resistor that can be added to change the gain of the tachometer input. See section below on Tachometer Gain for more details.

Tuning With Through-hole Components

In general, the drive will not need to be further tuned with through-hole components. However, for applications requiring more precise tuning than what is offered by the potentiometers and dipswitches, the drive can be manually modified with through-hole resistors and capacitors as denoted in the above table. By default, the through-hole locations are not populated when the drive is shipped. Before attempting to add through-hole components to the board, consult the section on loop tuning in the installation notes on the manufacturer's website. Some general rules of thumb to follow when adding through-hole components are:

- A larger resistor value will increase the proportional gain, and therefore create a faster response time.
- A larger capacitor value will increase the integration time, and therefore create a slower response time.

Proper tuning using the through-hole components will require careful observation of the loop response on a digital oscilloscope to find the optimal through-hole component values for the specific application.

Tachometer Gain

Some applications may require an increase in the gain of the tachometer input signal. This occurrence will be most common in designs where the tachometer input has a low voltage to RPM scaling ratio. The drive offers a through-hole location listed in the above table where a resistor can be added to increase the tachometer gain. Use the drive's block diagram to determine an appropriate resistor value.

†Note: Damage done to the drive while performing these modifications will void the warranty.

Appendix B:

Maxon

Motor, Gears and Encoder

EC 45 ∅45 mm, brushless, 150 Watt, CE approved

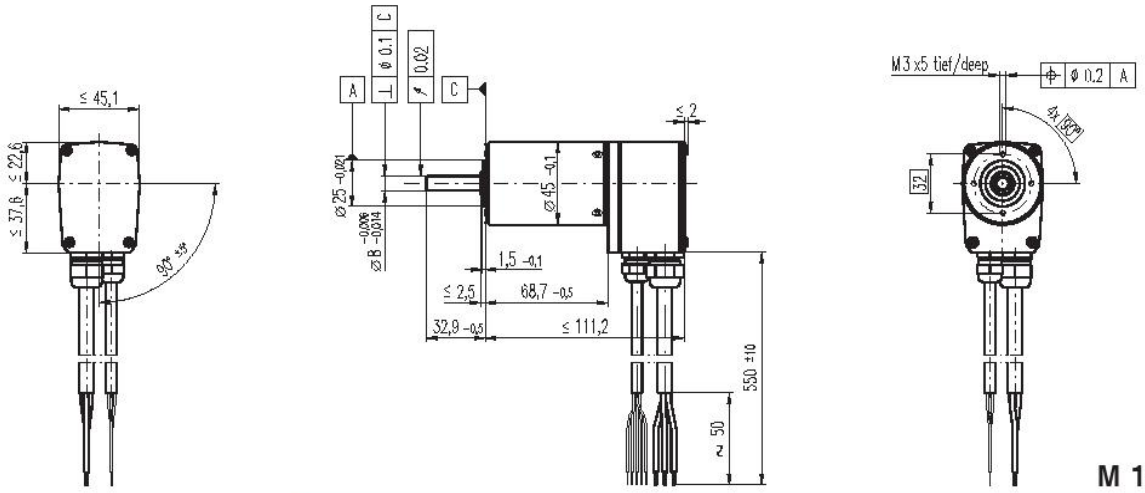

Stock program
Standard program
Special program (on request)

Order Number

		136202	136196	136203	136197	136204	136198	136205	136200	136206	136201
Motor Data											
	Values at nominal voltage										
1	Nominal voltage	V	12.0	12.0	18.0	18.0	24.0	24.0	36.0	36.0	48.0	48.0
2	No load speed	rpm	9770	5630	10300	5920	10500	6070	9340	5380	10100	5850
3	No load current	mA	1860	722	1350	522	1060	409	572	223	496	192
4	Nominal speed	rpm	8610	4430	9100	4710	9360	4860	8180	4200	8980	4650
5	Nominal torque (max. continuous torque)	mNm	168	182	165	181	163	179	174	188	168	183
6	Nominal current (max. continuous current)	A	16.0	9.61	11.1	6.69	8.45	5.10	5.24	3.13	4.16	2.51
7	Stall torque	mNm	1590	916	1650	955	1670	965	1590	916	1670	965
8	Starting current	A	138	45.8	100	33.4	78.0	26.0	43.8	14.6	37.6	12.5
9	Max. efficiency	%	79	77	79	77	79	77	79	77	79	77
	Characteristics											
10	Terminal resistance phase to phase	Ω	0.0873	0.262	0.180	0.539	0.308	0.923	0.823	2.47	1.28	3.83
11	Terminal inductance phase to phase	mH	0.0266	0.0797	0.0542	0.163	0.0917	0.275	0.263	0.788	0.395	1.19
12	Torque constant	mNm / A	11.5	20.0	16.5	28.6	21.4	37.1	36.3	62.8	44.5	77.1
13	Speed constant	rpm / V	827	478	579	334	445	257	263	152	214	124
14	Speed / torque gradient	rpm / mNm	6.25	6.25	6.30	6.30	6.39	6.39	5.97	5.97	6.16	6.16
15	Mechanical time constant	ms	7.79	7.79	7.86	7.86	7.97	7.97	7.44	7.44	7.67	7.67
16	Rotor inertia	gcm²	119	119	119	119	119	119	119	119	119	119

Specifications

	Thermal data	
17	Thermal resistance housing-ambient	1.9 K / W
18	Thermal resistance winding-housing	0.9 K / W
19	Thermal time constant winding	15 s
20	Thermal time constant motor	1600 s
21	Ambient temperature	-20 ... +100°C
22	Max. permissible winding temperature	+125°C
	Mechanical data (preloaded ball bearings)	
23	Max. permissible speed	15000 rpm
24	Axial play at axial load < 20 N	0 mm
	> 20 N	max. 0.14 mm
25	Radial play	preloaded
26	Max. axial load (dynamic)	20 N
27	Max. force for press fits (static)	170 N
	(static, shaft supported)	5000 N
28	Max. radial loading, 5 mm from flange	140 N
	Other specifications	
29	Number of pole pairs	1
30	Number of phases	3
31	Weight of motor	850 g
	Protection to	IP54

Values listed in the table are nominal.

Connection motor (Cable AWG 16)

Cable 1	Motor winding 1
Cable 2	Motor winding 2
Cable 3	Motor winding 3

Connection sensors (Cable AWG 24)

white	Hall sensor 3
brown	Hall sensor 2
green	Hall sensor 1
gelb	GND
grey	V_{Hall} 4.5 ... 24 VDC

Wiring diagram for Hall sensors see page 27

Option
Temperature monitoring, PTC resistance Micropille 110°C, R 25°C < 0.5 kΩ, R 105°C = 1.2 ... 1.5 kΩ, R 115°C = 7 ... 13 kΩ, R 120°C = 18 ... 35 kΩ,
Motor connection with plug

Operating Range

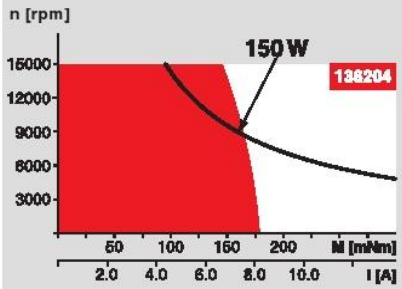

Comments

Continuous operation
In observation of above listed thermal resistance (lines 17 and 18) the maximum permissible winding temperature will be reached during continuous operation at 25°C ambient.
= Thermal limit.

Short term operation
The motor may be briefly overloaded (recurring).

Assigned power rating

maxon Modular System

Overview on page 16 - 21

Planetary Gearhead
∅42 mm
3 - 15 Nm
Page 240

Planetary Gearhead
∅52 mm
4 - 30 Nm
Page 243

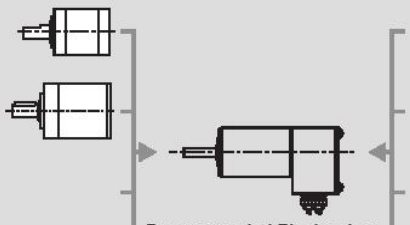

Recommended Electronics:

DECS 50/5	Page 288
DEC 50/5	289
DECV 50/5	295
DEC 70/10	295
DES 50/5	296
DES 70/10	296
EPOS2 50/5	303
EPOS 70/10	303
Notes	**20**

Encoder HEDL 9140
500 CPT,
3 channels
Page 273

Resolver Res 26
∅26 mm
10 V
Page 278

Brake AB 28
∅28 mm, 24 VDC
0.4 Nm
Page 317

Appendix C:

National Instruments

Motion Controller

High-Performance Stepper/Servo Motion Controllers

NI 735x

- Up to 8 axes of motion
- Configurable stepper or servo control
- Up to 4 MHz stepper output rate
- 62 µs PID loop update rate for up to 2 axes
- 3D linear and circular interpolation
- 3D contouring
- Sinusoidal commutation for brushless motors
- Buffered breakpoints for high-speed integration
- Patented step generation technology for smooth stepper motion

Operating Systems

- Windows Vista/XP/2000
- LabVIEW Real-Time

Recommended NI Software

- LabVIEW
- NI Motion Assistant
- LabWindows™/CVI
- Measurement Studio

Other Compatible Software

- Visual Basic
- C/C++

Driver Software (included)

- NI-Motion

Overview and Applications

NI 735x PCI and PXI stepper and servo motion controllers are for machine builders and users who need the highest performance and a high-axis count in a small space. The NI PXI-7358 is the first 8-axis stepper or servo motion controller packaged as a 1-slot 3U PXI module. It offers many advanced features, including sinusoidal commutation for brushless motors. NI 735x motion controllers are available in 2-, 4-, 6-, and 8-axis versions for PXI and PCI.

Motion Control and LabVIEW Real-Time

Many motion applications require very high reliability and integration with other types of I/O. NI PXI motion controllers are compatible with the NI LabVIEW Real-Time Module, with which you can create an integrated motion and I/O system that runs embedded in a real-time OS. A PXI motion controller with a PXI RT Series controller can run LabVIEW Real-Time and function as a stand-alone Ethernet-based motion controller. With this technology, you can create distributed motion control systems that integrate tightly with data acquisition or vision.

I/O Capabilities

NI 735x motion controllers have diverse I/O that is useful in many motion applications. You can use the 64 bits of digital I/O for a wide variety of applications such as opening or closing valves or turning on and off solid-state relays using the SSR adapter. These motion controllers also have eight channels of 16-bit analog I/O useful for reading potentiometers or other analog measurements.

Synchronizing Multiple Axes for Parallel Mechanism Applications

Because NI 735x controllers can control up to eight axes, they are ideal for high-axis parallel mechanisms where all axes need to be tightly synchronized. Using the NI-Motion driver software, you can start all axes at once and have each axis follow the acceleration and velocity profiles you have defined. This is useful when working with parallel mechanisms such as hexapods when the axes must move simultaneously.

Static-Friction Compensation

The frictional force present before an object starts moving is called static friction. Static friction is often higher than dynamic friction (frictional force present during motion) and if the difference between the two is large enough, it can make the system difficult to tune. The static-friction compensation feature of the NI 735x motion controllers compensates for this difference in friction for easier tuning and precise control. Piezoelectric systems exhibit high static friction and can benefit from the static friction compensation feature of the NI 7350 series motion controllers. In addition, to help you tune your system, NI offers the free Piezo Tuning Wizard. After tuning your system using the Piezo Tuning Wizard, you can easily program the system using LabVIEW software and NI Motion Assistant just as you would program any other system.

NATIONAL INSTRUMENTS™

Sinusoidal Commutation

Brushless servo motors require sinusoidal commutation. Although many advanced motor drives have built-in commutation capability, many lower-cost drives require the motion controller to provide commutation. With sinusoidal commutation, offered by the NI 7350, you can obtain the smoothest possible motion with a brushless servo motor and a lower cost drive.

Note that when using the sinusoidal commutation feature, use two axis resources for each drive you connect to. This is because two analog outputs are needed to provide the commutation.

Increasing Integration Speed with New Breakpoint and High-Speed Capture Enhancements

NI 7350 series motion controllers offer buffered breakpoints for precise timing between motion and measurements or vision. Using this feature, you can send a buffer of position breakpoints to the controller that trigger a digital signal upon reaching the positions in the buffer. Buffered breakpoints can trigger at rates as high as 2 kHz. For equally spaced positions, you can use periodic breakpoints to achieve even higher speeds of up to 4 MHz. With periodic breakpoints, you supply a position modulus. Each time the position reaches that modulus position, the breakpoint triggers. Another new feature that enhances integration speed is the new buffered high-speed position capture for NI 735x controllers. This feature captures positions based on a trigger from an external source or from a data acquisition or machine vision device. The high-speed capture can capture positions at rates of up to 2 kHz per axis.

Additional Features

For the NI 735x controllers, your PID update rate can be 62.5 µs for up to two axes. This means that for multiaxis applications, the PID rates can be twice as fast as those for previous boards. An NI 735x also has increased resolution for analog-to-digital conversion, giving you high resolution for analog position feedback.

Feature	NI 735x
Number of Axes	2, 4, 6, 8
PAC Platforms	PCI, CompactPCI/PXI
Linear, Circular, Spherical, and Helical Interpolation; Blending	0
Trapezoidal, S-Curve Profiles	0
Closed-Loop Stepper Control	0
Contouring, Electronic Gearing, Onboard Programming	0
Sinusoidal Commutation for Brushless Servo Motors	0
Buffered Breakpoints, Buffered High-Speed Capture, 4 MHz Periodic Breakpoints	0
Number of Axes per 62.5 µs PID Rate	2
PWM Lines/DIO Lines/Analog Input Resolution	2/64/16-bit
Maximum Step Output Rate/Encoder Input Rate	8 MHz/20 MHz
Programming API	NI-Motion Driver
Software	NI Motion Assistant, NI LabVIEW, C, Visual Basic

NI 7350 Motion I/O Connector Pinouts

(two 68-pin VHDCI connectors)

Axis 1 Dir (CCW)	1	35	Axis 1 Step (CW)
Digital Ground	2	36	Axis 1 Encoder Phase A
Digital Ground	3	37	Axis 1 Encoder Phase B
Axis 1 Home Switch	4	38	Axis 1 Encoder Index
Trigger 1	5	39	Axis 1 Forward Limit Switch
Axis 1 Inhibit	6	40	Axis 1 Reverse Limit Switch
Axis 2 Dir (CCW)	7	41	Axis 2 Step (CW)
Digital Ground	8	42	Axis 2 Encoder Phase A
Digital Ground	9	43	Axis 2 Encoder Phase B
Axis 2 Home Switch	10	44	Axis 2 Encoder Index
Trigger 2	11	45	Axis 2 Forward Limit Switch
Axis 2 Inhibit	12	46	Axis 2 Reverse Limit Switch
Axis 3 Dir (CCW)	13	47	Axis 3 Step (CW)
Digital Ground	14	48	Axis 3 Encoder Phase A
Digital Ground	15	49	Axis 3 Encoder Phase B
Axis 3 Home Switch	16	50	Axis 3 Encoder Index
Trigger 3	17	51	Axis 3 Forward Limit Switch
Axis 3 Inhibit	18	52	Axis 3 Reverse Limit Switch
Axis 4 Dir (CCW)	19	53	Axis 4 Step (CW)
Digital Ground	20	54	Axis 4 Encoder Phase A
Digital Ground	21	55	Axis 4 Encoder Phase B
Axis 4 Home Switch	22	56	Axis 4 Encoder Index
Trigger 4	23	57	Axis 4 Forward Limit Switch
Axis 4 Inhibit	24	58	Axis 4 Reverse Limit Switch
Digital Ground	25	59	Host +5 V
Breakpoint 1	26	60	Breakpoint 2
Breakpoint 3	27	61	Breakpoint 4
Digital Ground	28	62	Shutdown
Analog Output 1	29	63	Analog Output 2
Analog Output 3	30	64	Analog Output 4
Analog Output Ground	31	65	Reserved
Analog Input 1	32	66	Analog Input 2
Analog Input 3	33	67	Analog Input 4
Analog Reference (Output)	34	68	Analog Input Ground

Motion I/O Connector for Axes 1-4

Axis 5 Dir (CCW)	1	35	Axis 5 Step (CW)
Digital Ground	2	36	Axis 5 Encoder Phase A
Digital Ground	3	37	Axis 5 Encoder Phase B
Axis 5 Home Switch	4	38	Axis 5 Encoder Index
Trigger 5	5	39	Axis 5 Forward Limit Switch
Axis 5 Inhibit	6	40	Axis 5 Reverse Limit Switch
Axis 6 Dir (CCW)	7	41	Axis 6 Step (CW)
Digital Ground	8	42	Axis 6 Encoder Phase A
Digital Ground	9	43	Axis 6 Encoder Phase B
Axis 6 Home Switch	10	44	Axis 6 Encoder Index
Trigger 6	11	45	Axis 6 Forward Limit Switch
Axis 6 Inhibit	12	46	Axis 6 Reverse Limit Switch
Axis 7 Dir (CCW)	13	47	Axis 7 Step (CW)
Digital Ground	14	48	Axis 7 Encoder Phase A
Digital Ground	15	49	Axis 7 Encoder Phase B
Axis 7 Home Switch	16	50	Axis 7 Encoder Index
Trigger 7	17	51	Axis 7 Forward Limit Switch
Axis 7 Inhibit	18	52	Axis 7 Reverse Limit Switch
Axis 8 Dir (CCW)	19	53	Axis 8 Step (CW)
Digital Ground	20	54	Axis 8 Encoder Phase A
Digital Ground	21	55	Axis 8 Encoder Phase B
Axis 8 Home Switch	22	56	Axis 8 Encoder Index
Trigger 8	23	57	Axis 8 Forward Limit Switch
Axis 8 Inhibit	24	58	Axis 8 Reverse Limit Switch
Digital Ground	25	59	Host +5 V
Breakpoint 5	26	60	Breakpoint 6
Breakpoint 7	27	61	Breakpoint 8
Digital Ground	28	62	Shutdown
Analog Output 5	29	63	Analog Output 6
Analog Output 7	30	64	Analog Output 8
Analog Output Ground	31	65	Reserved
Analog Input 5	32	66	Analog Input 6
Analog Input 7	33	67	Analog Input 8
Analog Reference (Output)	34	68	Analog Input Ground

Motion I/O Connector for Axes 5-8

NI 7350 Digital I/O Connector Pinouts

(two 68-pin VHDCI connectors)

+5 V	1	35	Digital Ground
PCLK	2	36	Digital Ground
Reserved	3	37	Digital Ground
Reserved	4	38	DPull (P1:P4)
PWM1	5	39	Digital Ground
Reserved	6	40	Reserved
Reserved	7	41	Digital Ground
Reserved	8	42	Digital Ground
PWM2	9	43	Digital Ground
Port 1:bit 0	10	44	Port 1:bit 1
Ground	11	45	Port 1:bit 2
Port 1:bit 3	12	46	Digital Ground
1:bit 4	13	47	Port 1:bit 5
Digital Ground	14	48	Port 1:bit 6
Port 1:bit 7	15	49	Digital Ground
Port 2:bit 0	16	50	Digital Ground
2:bit 1	17	51	Port 2:bit 2
Digital Ground	18	52	Port 2:bit 3
Digital Ground	19	53	Port 2:bit 4
Ground	20	54	Port 2:bit 5
Port 2:bit 6	21	55	Digital Ground
Port 2:bit 7	22	56	Digital Ground
3:bit 0	23	57	Port 3:bit 1
Digital Ground	24	58	Port 3:bit 2
Port 3:bit 3	25	59	Digital Ground
3:bit 4	26	60	Port 3:bit 5
Digital Ground	27	61	Port 3:bit 6
Port 3:bit 7	28	62	Digital Ground
4:bit 0	29	63	Port 4:bit 1
Digital Ground	30	64	Port 4:bit 2/Axis 1, Hall 1
Axis 1, Hall 2/Port 4:bit 3	31	65	Digital Ground
Axis 1, Hall 3/Port 4:bit 4	32	66	Port 4:bit 5/Axis 2, Hall 1
Digital Ground	33	67	Port 4:bit 6/Axis 2, Hall 2
Axis 2, Hall 3/Port 4:bit 7	34	68	Digital Ground

Digital I/O Connector for Axes 1-4

+5 V	1	35	Digital Ground
Reserved	2	36	Digital Ground
Reserved	3	37	Digital Ground
Reserved	4	38	DPull (P5:P8)
Reserved	5	39	Digital Ground
Reserved	6	40	Reserved
Reserved	7	41	Digital Ground
Reserved	8	42	Digital Ground
Reserved	9	43	Digital Ground
Port 5:bit 0	10	44	Port 5:bit 1 Digital
Digital Ground	11	45	Port 5:bit 2
Port 5:bit 3	12	46	Digital Ground Port
Port 5:bit 4	13	47	Port 5:bit 5
Digital Ground	14	48	Port 5:bit 6
Port 5:bit 7	15	49	Digital Ground
Port 6:bit 0	16	50	Digital Ground Port
Port 6:bit 1	17	51	Port 6:bit 2
Digital Ground	18	52	Port 6:bit 3
Digital Ground	19	53	Port 6:bit 4 Digital
Digital Ground	20	54	Port 6:bit 5
Port 6:bit 6	21	55	Digital Ground
Port 6:bit 7	22	56	Digital Ground Port
Port 7:bit 0	23	57	Port 7:bit 1
Digital Ground	24	58	Port 7:bit 2
Port 7:bit 3	25	59	Digital Ground Port
Port 7:bit 4	26	60	Port 7:bit 5
Digital Ground	27	61	Port 7:bit 6
Port 7:bit 7	28	62	Digital Ground Port
Port 8:bit 0	29	63	Port 8:bit 1
Digital Ground	30	64	Port 8:bit 2/Axis 3, Hall 1
Axis 3, Hall 2/Port 8:bit 3	31	65	Digital Ground
Axis 3, Hall 3/Port 8:bit 4	32	66	Port 8:bit 5/Axis 4, Hall 1
Digital Ground	33	67	Port 8:bit 6/Axis 4, Hall 2
Axis 4, Hall 3/Port 8:bit 7	34	68	Digital Ground

Digital I/O Connector for Axes 5-8

Ordering Information

NI PXI-7358 (8-axis) 778540-08
NI PXI-7356 (6-axis) 778540-06
NI PXI-7354 (4-axis) 778540-04
NI PXI-7352 (2-axis) 778540-02
NI PCI-7358 (8-axis) 778440-08
NI PCI-7356 (6-axis) 778440-06
NI PCI-7354 (4-axis) 778440-04
NI PCI-7352 (2-axis) 778440-02

Includes NI-Motion software libraries and examples.

Accessories

NI Motion Assistant 778553-01

Wiring Interfaces

NI UMI-7764.....777978-02 NI
UMI-7772.....778556-01 NI
UMI-7774.....778558-01

Power Drives

NI MID-7604.....777936-01 NI
MID-7602.....778003-01 NI
MID-7654.....778005-01 NI
MID-7652.....778004-01
P70530 780097-01
P70360 780098-01

BUY NOW!

For complete product specifications, pricing, and accessory information, call 800 813 3693 (U.S.) or go to **ni.com/info**andenter **ni7350**.

Specifications

Performance

PID update rate range..... 62.5 to 500 µs/sample
- Maximum PID update rate ..... 62.5 µs/axis
- 8-axis PID update rate..... 250 µs total

Multiaxis synchronization..... <1 update sample

Trajectory parameters
- Absolute position range ..... $\pm 2_{31}$ counts
- Maximum relative move size ..... $\pm 2_{31}$ counts
- S-curve time range ..... 1 to 32,767 samples
- Following error range ..... ±32,767 counts
- Velocity range ..... Servo: 1 to ±20,000,000 counts/s
- Velocity range ..... Stepper: 1 to 8,000,000 steps/s
- Acceleration/deceleration..... 244 to 512,000,000 counts/s_2 at a PID rate of 250 µs
- Gear ratio..... ±32,767:1 to ±1:32,767

Servo control loop modes ..... PID, PIVff, S-curve, dual loop
- PID (Kp, Ki, and Kd) gains..... 0 to 32,767

Stepper outputs
- Maximum pulse rate ..... 8 MHz (full, half, and microstep)
- Minimum pulse width ..... 50 ns at >4 MHz
- Step output mode ..... Step and direction or CW/CCW
- Voltage range ..... 0 to 5 V

System Safety

Watchdog timer function..... Resets board to startup state

Shutdown input..... Disable all axes and command outputs

Motion I/O

Servo command analog outputs
- Voltage range ..... ±10 V, 16 bits (0.000305 V/ LSB)
- Programmable torque (velocity) limits and programmable offset..... ±10 V (-32,768 to +32,767)

Encoder inputs ..... Quadrature, incremental, single-ended
- Maximum count rate ..... 20 MHz

Forward, reverse, and home inputs
- Number of inputs..... 24 (3 per axis)
- Control ..... Individual enable/disable, stop on input, prevent motion, find reference

Trigger (position capture) inputs..... 8 (one per axis)
- Maximum buffered capture $rate_1$... 2 kHz per axis

Breakpoint (position compare) outputs.. 8 (one per axis), programmable polarity
- Maximum periodic rate ..... 4 MHz
- Maximum buffered trigger $rate_1$ .... 2 kHz per axis

Inhibit/enable output ..... 8 (one per axis), programmable polarity

Analog inputs..... up to 8, 16-bit resolution, ±10 V range, 25 µs scan rate

Analog outputs..... 8, 16-bit resolution, ±10 V range

1Assumes a PID update rate of 250 µs. 2 kHz per axis for PID rates between 62.5 and 250 µs, and 1 kHz per axis for PID rates greater than 250 µs. This value must not exceed 8 kHz total for all ongoing buffered breakpoint (position compare) and trigger (position capture) operations.

Digital I/O

Ports ..... 8, 8-bit TTL ports, bit configurable, sink or source 24 mA outputs

Open-loop PWM outputs
- Number of PWM outputs ..... 2, 50 kHz
- Clock sources..... Internal or external

Power Requirements

+3.3 V (±10%)..... 2A
+5 V (±5%)..... 2A
+12 V (±5%)..... - 30 mA 0
12 V (±10%) ..... mA
Power consumption ..... 18 W, maximum

Physical

Dimensions (not including connectors)
- PXI..... 16 by 10 cm (6.3 by 3.9 in.)
- PCI..... 17.5 by 9.9 cm (6.9 by 3.9 in.)

Connectors
- Motion I/O connector ..... 68-pin female high-density VHDCI type
- Digital I/O connector ..... 68-pin female high-density VHDCI type

Environment

Operating temperature ..... 0 to 55 °C
Storage temperature..... -20 to 70 °C
Relative humidity range..... 10 to 90% (noncondensing)

Appendix D:

Photographs of Prototype

One-module prototype before movement

One-module prototype after movement

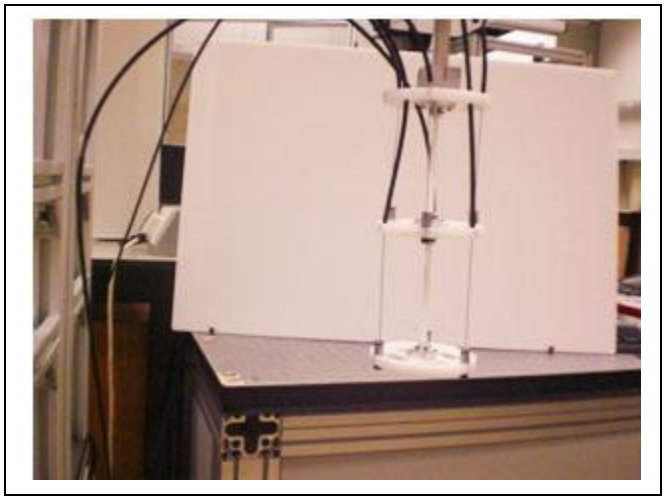

Two-module prototype before movement

Two-module prototype after movement